Author Response:

We thank the reviewers for their valuable comments and suggestions. We have incorporated majority of their suggestions, which greatly improved the quality of the manuscript. The specific response to the reviewer's queries are addressed.

Below we listed the major changes that have been made in the revised version of the manuscript.

- The data referred to as Swv (19 samples) are not included in the revised manuscript. The meteorological parameters which were measured at the height of 15m above the surface of the ocean and not at the height at which Swv samples were collected (which was close to the ocean surface during calm conditions).
- The stucture of the paper is modified. The explanation of the the Unified and the Traditional Craig-Gordon models and the HYSPLIT back trajectory analysis has been moved to the methods section.
- The models are run for the turbulent indices (x) of 0-1 with an increment of 0.1. In the old manuscript we had run the models for only 0, 0.5 and 1.
- Most of the figures are modified to include the new results from modelling experiments and a few additional figures were included. All these figures with modified captions are presented in the main manuscript and the revised supplememtary document.
- 4 new tables were also included in the revised submission. Two of these tables are presented in the manuscript and two in supplementary document.

Response to Reviewer 1

Below we have compiled our answers to the reviewer's questions and comments.

Please note that the Swv samples were excluded in the modified manuscript as lack meteorological parameters for them. Therefore only samples Nwv at the sampling height of 15m were taken for the paper.

The reviewer's comments and questions are presented as italic while our answers are written as bold.

The paper presents isotopic water vapor and meteorological data collected during two 'summer' cruises on RV S.A. Agulhas in 2017-2018 is the Indian Ocean sector of the southern Ocean. The sample data are not numerous, but are very valuable, as meteorological conditions are well described and cover a large spread of conditions. The paper attempts two things: first to check the local equilibrium assumption that atmospheric water vapor results from local sea water evaporation using two models (TCG and UCG), and then attempts to find where and why this breaks down (in the southern part with continental air outflow). The approach is valuable, but should be much more clearly outlined. For example, lines 40-45 of the introduction should be expanded and it should be made clearier what is the approach adopted. This should be reminded at the beginning of the discussion 4 (line 143), so that the reader does not have to wait on lines 219-220 to understand what is the approach followed (first 'local' evaporation, thus the equilibrium model; then, remote/mixing contributions).

The introduction is now modified for clarity with more description on the approach adopted in the study.

When assuming local evaporation, the abstract and conclusion state that the UCG model with a 0.5 CD molecular diffusivity ratio performs best. I find that conclusion not substantiated, and believe that there are cases with TCG which perform as well. This could be clarified.

In the modified version of this study, the Craig-Gordon models (both UCG and TCG) were run for different fractions of the turbulent indices, x (i.e. the fraction of molecular and turbulent diffusion). The value of x was varied from 0 to 1 with an interval of 0.1. We found that the UCG and TCG models both perform well for MJ and CD molecular diffusivity ratios, while for the PW diffusivity ratios the difference between the observed and the modelled values is the largest. This is explained in the paper. We found that UCG MJ for x=0.8, UCG CD for x=0.6 and TCG MJ for x=0.6 and TCG CD for x=0.7 perform equally well within the uncertainty limits.

The main issues I have are the followings:
1: how well were meteorological parameters measured (in particular, for relative humidity, and was this measurement done very close to where the air was collected (upper level). I find the very large relative humidities in the southern part of the first cruise transect surprising in view of the much weaker relative humidities of the second cruise. Of course, this is possible, but would suggest, almost fog-like conditions for the first cruise. If this is the case, this could involve very different processes and thus expected isotopic properties of the near-surface air mass (what type of clouds, then; subsidence or not?)

The meteorological parameters were measured at the height of ~15 m from sea level, which was the sampling inlet for water vapour isotopic measurements. The relative humidity was estimated at the dry and the wet bulb temperature using the psychrometric charts. The two

cruises differs in the latitudinal coverage area. Water vapour sampling in the first cruise was carried out until 69.3°S, whereas for the second cruise, the sampling was conducted until 66.8 °S. We recorded continuous precipitation over a duration between 20/01/2017-25/01/2017 (SOE IX) when relative humidity level approached higher values.

2. *The meteorological situations are described in ways which are too vague. For example, names of regions a little strange on lines 82-86 (for example melting/freezingstarting at 47 ◦ S?) On what is it based? What does it represent? I think that the different situations: cyclonic/ anticyclonic/ precipitating systems, presence of rain or snow should all be also reported and analyzed to provide a more relevant context that just the HYPSLIT trajectories, which as they are triplets are very hard to read as presented(and are not really commented upon. . .). Also, in which conditions were the high-winds encountered.*

This section is now modified.
The triplet HYSPLIT trajectories are shown together to give comprehensive overview about the overall moisture transport pathways.
The Southern Ocean is generally associated with high wind speed conditions.

3: *I was surprised to find why the (local equilibrium) model fit seem to work less well with the near surface samples. Any explanation for that? Alltogether, how samples are collected at the two levels should be more clearly described (maybe in supplementary materials, see comments below). Otherwise, it is very hard to understand what to make of the differences in results for the two sets of data.*

The meteorological parameters which goes as input parameters are measured at the height of ~15 m. This would be one of one of the major reason responsible for the discrepancy between near surface samples (Swv) and the samples collected at ~15m above the ocean surface.

- **Therefore, the Swv samples have been omitted from discussion.**
- **Additional information on the sampling procedures has been added in the supplementary document.**
- **The Swv samples were collected when the ocean surface conditions were calm i.e. when there was no visible wave in the ocean (No wave breaking near the sampling inlet and the ship was kept stationary for conducting the CDT depth profiling and sampling. The ocean beyond 65S latitude was relatively calm as compared to other latitudes.**

I will now provide a few comments on the figures:

Figure 1 : What are the white circles (compared to all the other red circles) ?

- **The white circles depict the locations of the water vapour (Swv) samples i.e. the vapour samples collected close to the ocean surface by placing the inlet tube just 1 m above the Sea water level. Since these samples were omitted from the discussion now, the figure has been modified and the caption has been rewritten to accommodate the new changes. (Figure 1 in the manuscript)**

Caption figure 2, last sentence: 'Read and blue colors. . . temperature, respectively.' It is hard to differentiate the two colors. Maybe air temperature should be open dots with no color inside?

- **The figure has been modified according to the suggestion. (Figure 2 in the manuscript)**

Figure 2 suggests that average conditions were with much less relative humidity at high latitudes during second cruise than during the first one. What is the big difference between the two cruises. I find relative humidity so high and for so long on SOE-IX (first cruise) a bit surprising.

- **There was continuous cloud cover for the days with high RH levels. Also, precipitation event lasted for the entire length with low pressure system as mentioned earlier.**

In particular, this does not seem to be so substantiated by figure 3, but I don't read very well figure 3, which I don't find very clear.

- **The triplet HYSPLIT trajectories are shown together to give comprehensive overview about the overall moisture transport pathways. There exists a few cases for both the expeditions when there was a complete mismatch between the observed and the HYSPLIT predicted RH values (governed by the Reanalysis dataset). The RH along the back-trajectories in close to 0 for all elevations. This may be due to missing data values in the input dataset used for generating the HYSPLIT model results.**

It does not seem either the values that are retained afterwards for humidity (such as in figure 6). Have they been adjusted afterwards?

- **In the old Figure 6, samples collected exclusively north of 65S latitude were plotted. The reason being the mixing of Antarctic vapor with depleted heavy isotope values south of 65S latitude. Large relative humidity were mostly observed for the region south of 65S and during the passage of an extratropical cylone. This figure has been modified to include all the data points and the regression equations for various sample classifications have been provided in a separate table.**

Figure 4, top panel a) suggest south of 40 ◦ S SOE-X lower than SOE-IX, itself lower than SW global database. It is a bit surprising, but could be associated with different surface salinities and freshwater sources. What are the salinities and how do they compare with surface water isotopic composition; differences between the two cruises?

- **The cruises were not during the same month, for SOE IX the sampling was performed in January 2017 while for SOE-X the samples were collected during December-2017 to mid January-2018 . The salinity values measured along the transect are now included in the revision.**

For figure 4, b), d18O SOE-IX and SOE-X seem rather similar, except maybe some d18O Swv de SOE-X, which could be a little higher near 40-50 ◦ S. For dxs less obvious. I don't see a clear (panel c) difference in dxs near 45-65 ◦ S between the two cruises, despite very different relative humidities? (big apparent jump near 45 ◦ S).

- **The Swv samples is now removed from the modified figure.**
- **In addition to the local factors, the dxs is also controlled by the mixing of the advected vapor this is probably the reason.**

Last sentence of the caption of Figure 4: This is not just zonal variation, but maybe statistical distributions grouped by latitudinal bands.

- **Latitudinal ranges (Zones) are grouped according to the approximate positioning of the general wind patterns (easterly or westerly) decided based on the HYSPLIT trajectories. The caption has been modified to make the idea clear.**

Figure 5: dependency in humidity seems dubious, but could it be poor measurements and would'nt it be then important to separate the cruises (issue also of cross wind-dependency) Water samples south of 65 ◦ S clearer, as well as Swv wamples (but very scattered and how does one measure those).

- **We agree the plot is confusing, the plot has been modified and some information has been provided in the tables (Table 1S for d18O and Table 2S for d2H). The relationships for separate cruises has been added.**

- **The sampling for Swv water vapor samples was totally dependent on the ocean conditions encountered. The dependency might be dubious to some extent as the measurements for relative humidity were done at the height of the Nwv samples (~15m above the sea level).**
- **The Swv samples have not been included in the modified version of the manuscript due to the reasons stated before.**

Plot on b) dependency of SST is clearly wrong panel (not right SST! And same clearly as for a; this raises issues of whether one trusts fully the other figures).

- **I don't understand this question. Nevertheless, this figure has been modified and additional information has been added in Table 1S and Table 2S.**

Figure 6 on d-excess dependency and meteorological conditions seem rather in agreement (north of 65 ◦ S) with Uemura et al. (2008) (also a bit shifted down compared to Uemura's values which could suggest an average bias in one of the data sets).

- **This is due to the fact that low temperatures (both sst and air temperatures) are low beyond 65S and hence limit the evaporation. Moreover, beyond 65S there is advection and mixing of very light Antarctic vapor.**
- **This really answers the doubt you raised and clears it regarding the dubiousness of RH measurements. It has been mentioned in the text that if considered separately the relationship is stronger and -0.64h+ 57.4‰ (r2 =0.77) and -0.64h+48.7 (r 2 =0.61) for SOE IX and SOE X respectively comparable to the that from previous measurements in the Southern Ocean (Uemura et al. 2008) -0.61h+55.71(r2=0.63).**
- **The figure has been modified and the additional information has been provided in a table (Table 2)**

Figure 7. UCG presents some strange peaks. Why? That could be an argument for preferring TCG, but I don't know how realistic the different ocean surface conditions selected are. On this figure, there is no particular need for the colors of the diamonds

- **The larger variability for in the isotopic values predicted by the both UCG and TCG models for MJ and CD molecular diffusivity ratios and thus maybe a reason for a better representation of the conditions under which evaporation happens in the open ocean by CG models for these molecular diffusivity ratios. The model runs for different molecular diffusivity ratios have been separated in the modified figure and are much clearer now.**
- **The ocean conditions x (turbulence coefficient) are selected are assuming ratios of molecular (x=1) to turbulent transport (x=0) and x=0.5 for equal contribution by molecular and turbulent diffusion. In the modified version the models are run for x varying from 0-1 with an increment of 0.1.**
- **This figure has been modified and the data are presented separately for d18O and d-excess. (Figure 7 shows the comparision between modelled and observed d18O and Figure 8 between modelled and observed d-excess)**

Figure 8: interesting. Actually, both UCG and TCG models don't explain observed d-excess at humidity larger than 90%. Otherwise, dependency in SST and wind speed seem OK for both (TCG gives a reduced range compared to UCG, so should the results be considered better?). Some cases better both in term of correlation and small misfits in slope and intercept.

- **This is a known shortcoming of the model as it doesn't perform well for high RH conditions, where greated influence on the isotopic composition is exerted by the advected vapor.**

- **During the period of sampling, high RH conditions were observed when precipitation occurred and when extratropical cyclones were encountered (as evident from the low pressures).**
- **In the modified version as explained before, it was found that UCG MJ for x=0.8, UCG CD for x=0.6 and TCG MJ for x=0.6 and TCG CD for x=0.7 perform equally well within the uncertainty limits. The comparision between the observed and these models have been added as a separate figure. (Figure 10)**
- **The models that best describe the conditions are selected for which there are least differences between the regression parameters (slope and intercept) of the meteorological parameters (rh, sst and wind speed) vs d-excess of water vapor. (Figure 9, Figure 11 and Figure 12)**

(figure 9; the caption should mention whether the comparisons are done with UCG or TCG). The different curves and what they mean (their caption) are hard to read on figures 7 to 10.

- **The comparisons have been presented for both UCG and TCG models. Since in the modified version, the models have been run for x varying between 0-1 with and increment of 0.1 as opposed to 0,0.5 and 1 in the previous version. This additonal information has been clearly presented in Figure 9, Figure 11 and Figure 12 in the modified version.**

Figure 10, probably interesting, but very hard to understand what is presented. Caption should be clearer, and as is does not explain what is presented. The yellow and green bars are too difficult to separate, and should be presented separately (for example one above the other)

- **Noted. The figure has been modified, all the model runs which perform well have been included and the caption rephrased. (Figure 13 and Figure 14 in the revised manuscript)**

In Supplementary material, presenting d18Osw is instructive, but it would be good to add a salinity column to increase the possible use of these data (the data were collected from a rosette with a Seabird CTD, so salinity was measured). It can also help validity-controlling the isotopic sea water data. For example, there is an isolated very negative value: if salinity low and/or collected near an iceberg, it is possible. Otherwise, questionable.

- **There were two ways the surface water samples were collected. The CTD, when the ship was kept stable for the stations where the depth sampling was being done and from a bucket thermometer when the ship was moving.**
- **The salinity values were measured from the CTD during the stations and 6 hourly using an AutoSalinometer during the whole period of the expeditions taking samples from the bucket thermometer.**
- **For the depth sampling stations, the salinity and the isotopic composition is from the same sample. Whereas, in most of the cases, when the ship was moving the surface water samples for mesuring the isotopic composition of the are not same as the ones for which the salinity was measured. Nevertheless, the surface salinity values from the Autosalinometer which were measured along the sampling transect have been plotted in Fig. 4a.**
- **The salinity values have been added and the sample with a negative was in fact collected near the iceberg. The other probable reason for the negative value is the freshwater mixing of precipitation as this sample was collected during the passage of a low pressure system.**

Detailed (mostly minor or editorial) comments:
Line 53: '. . . shows the sampling locations. ' How is Swv collected: at which height above the sea surface? How is spray avoided whether it is for Swv or Nwv. . .) .The detail of the collection method

could be key for the results obtained. Later, it is mentioned that Swv samples could only be collected by fair weather. What kind of wind/swells/sea states are conductive to this measurement. All these relevant informations should be provided in the supplementary document.

- **Swv samples have not been discussed in the modified version due to the reasons stated before.**
- **This information has been included in the supplementary document.**

l. 72 '. . ., the change between trajectories corresponding to trade winds from the ones corresponding to westerlies happened at 31 ◦ S, whereas at 630S, a change. . .'

- **Done**

l. 106: the sentence 'The role of sst in governing d-excess. . .' This is only direct role, there is the indirect one of the air water mass and dependency on temperature.

- **Noted. The sentence has been rephrased**

l. 113: 'The strength of the correlation is slightly higher. . .'

- **Done**

l. 120: more sensitivity of ï Ad'H to wind speed is not what comes out clearly from figure 5b. It might be a scaling issue of the ï Ad'18O versus ï Ad'D (note that R-square are small for both variables)

- **Noted, the sentence has been omitted.**

Line 129, the slope is the opposite in this latitude range between the two expeditions. This illustrates, I believe, either very different weather conditions (as seen in r of figure 2) or some issue somewhere, which would need to be further clarified

- **This was a typing error the values of slopes are in fact same for both the expeditions.**

Line 132? Sentence?

- **The sentence has been rephrased**

l. 134: '. . . complement. . .'

- **Done**

Line 135: correlation with SST of d18OSwv. Interesting, but these samples only taken when sea state not strong. Relating the dxs of seawater with relative humidity is a bit strange, as this is close to sea surface but with little wind/sea. I am not sure of what that brought?

- **As explained earlier, the conditions deemed feasible for sampling close to the surface were constrained by the ocean surface conditions. In order to completely minimise the influence of sea spray on the water vapour samples. As mentioned before, since the meteorological measurements were done at the height of 15m the discussion on Swv samples hasn't been included in the modified version of the manuscript.**
- **We haven't compared the dxs of seawater with relative humidity.**

l. 140: '. . . to the near-surface water vapour. . .' I am wondering whether the regression is significant, and in that case, whether this sentence is not anecdotical, and should be omitted.

- **The sentence has been omitted.**

In description of UCG (l. 157-191), the ratio term is ï A ˛ğ-h, which makes sense in this context. However, note that at saturation (fog, for example), thre is a definition issue. For that, The near saturation values reported on Figure 2 almost everywhere south of 50 ◦ S during SOE-IX is a major

issue. How was this dealt with (and again, what confidence does one have in these near-saturated conditions, not witnessed the second year).

- **As mentioned before, these were the conditions observed during the passage of low pressure systems as seen from the atmospheric pressure measurements.**

Line 175: remove a 'same'. After that, the global closure is assumed as in Merlivat (1978)

- **Done**

l. 201. I would mention the caveat of the issue of sea spray for high winds. Evaporation from sea spray is a large contribution to total evaporation in these conditions, and follows different laws (in the extreme case of all sea spray evaporating, this would for example yield Rev=Rl) There is also the caveat of below freezing temperature, and low SST close to sea ice formation temperature (just below fresh water freezing points), but I gather from figure 2 that this almost did not happen (correct?)

- **We have no way of knowing the fraction of sea spray contributing to the local moisture or whether all the sea spray that is formed is evaporating. So we have not discussed the influence of sea spray.**

l. 219-220. This sentence is key. I think that this should be presented earlier.

- **Done**

l. 229: '. . . where westerlies dominate. . .'

- **Done**

L. 233: end of sentence missing

- **Sentence rephrased**

l. 236 '. . . is less, and is largely local. . .'

- **Done**

Response to Reviewer 2

The submitted paper by Dar et al presents an analysis of isotopic data from southern latitudes. These data are compared with a set of models and associated coefficients. While worthwhile, a revision of the structure and error analysis of conducted here would greatly improve this submission.

The structure of the paper has been modified according to the suggestions and error analysis included. The standard errors in both slope and intercept have been mentioned where ever the regression analysis has been done. The root mean square errors and the standard error for the model vs observed comparisions have been included.

First, the overall structure of this paper is a bit jumbled. Much of the discussion material about the CG models should be moved into the methods section. Similarly, the discussion of how the HYSPLIT back trajectories were ran should also be described in the methods section.

The stucture has been modified according to the suggestions.

Second, the error analysis needs to be more fully documented. The testing of different model formulations and parameters is helpful, however the authors do not fully evacuate the errors and biases associated with each model. A more rigorous description of errors across all variables is needed. Finally, is there an optimal set of an parameters that others should use (i.e. what value of x and fractionation factors minimizes errors and bias)?

- **The error and biases associated with each model are well known and described in the number of previous studies, for e.g. The isotopic composition of atmospheric vapour is a factor responsible for the larges uncertainty in the model. Since our observations are mostly over the ocean AT 15 M LEVEL we have taken the global closure assumption i.e. the isotopic composition of atmospheric vapour is equal to the isotopic composition of evaporating water.**
- **In the modified version the performance of the models evaluated for different turbulence indices (i.e. the ratios of molecular and turbulent diffusion). The models were run for the values of x ranging from 0-1 with an increment of 0.1. We found that while the MJ and CD diffusivity ratios perform equally well for both the models, the PW values show the greater difference between the observed and modelled values.**
- **We found that UCG MJ for x=0.8, UCG CD for x=0.6 and TCG MJ for x=0.6 and TCG CD for x=0.7 perform equally well within the uncertainty limits.**

L4: Add latitudes numbers here.

- **Done**

L5: Reword the sentence that starts "The inter annual", its not clear what your trying to say

- **The sentence has been rephrased**

L19: Nearly and your double tilde are redundant.

- **This has been removed.**

L25: Missing an 'A' at the beginning?

- **Done**

L52: Define what you mean here by boundary later? Where these really at the boundary layer?

- **The sentence has been removed as the Swv samples have been omitted from the modified version of the manuscript.**

L65: This text on HYSPLIT methods should move to section 2.

- **Done**

L76: Careful with your terminology here. A positive delta value signifies that it was more enriched in heavy isotopes relative to VSMOW only.

- **The sentence has been rephrased.**

L110-L120 What are the significance and or uncertaintie3s of these regressions.

- **This information has been added to the table**

L132: Why not put the regression coefficients and stats from Figs 5 & 6 in a table

- **Done**

L143-201: This needs to all move to methods.

- **Done**

L197: Please directly state the numbers you used here for the diffusivities

- **Done**

L209: While differences between the slopes and intercepts are interesting, a more error though analysis should be conducted. What is the overall bias associated with each model, what are the root mean squared errors, etc.

- **The standard errors and root mean squared errors have been added in form of a table (Table 3)**

Craig-Gordon model validation using stable isotope ratios in water vapor over the Southern Ocean

Shaakir Shabir Dar[1], Prosenjit Ghosh[1,2], Ankit Swaraj[2], and Anil Kumar[3]

[1]Centre for Earth Sciences, Indian Institute of Science, Bengaluru, 560012, Karnataka, India.
[2]Divecha Centre for Climate Change, Indian Institute of Science, Bengaluru, 560012, Karnataka, India.
[3]National Centre for Polar and Ocean Research, Vaso-da-Gama, 403804, Goa, India.

Correspondence: Prosenjit Ghosh (pghosh@iisc.ac.in)

Abstract. The stable isotopic composition of water vapor over the ocean is governed by the isotopic composition of surface water, ambient vapor isotopic composition, exchange and mixing processes at the water-air interface as well as the local meteorological conditions. These parameters form inputs to the Craig-Gordon models, used for predicting the isotopic composition of vapor produced from the surface water due to the evaporation process. In this study we present water vapor, surface water isotope ratios and meteorological parameters across latitudinal transects in the Southern Ocean (27.38°S to 69.34°S and 21.98°S to 66.8°) during two austral summers. The performance of Traditional Craig-Gordon (TCG) (Craig and Gordon, 1965) and the Unified Craig-Gordon (UCG) (Gonfiantini et al., 2018) models is evaluated to predict the isotopic composition of evaporated water vapor flux in the diverse oceanic settings. The models are run for the molecular diffusivity ratios suggested by (Merlivat, 1978) (MJ), (Cappa et al., 2003) (CD) and (Pfahl and Wernli, 2009) (PW) and different turbulent indices (x) i.e. fractional contribution of molecular vs turbulent diffusion. It is found that the $UCG^{MJ}_{x=0.8}$, $UCG^{CD}_{x=0.6}$, $TCG^{MJ}_{x=0.6}$ and $TCG^{CD}_{x=0.7}$ models predicted the isotopic composition that best matches with the observations. The relative contribution from locally generated and advected moisture is calculated at the water vapor sampling points, along the latitudinal transects, assigning the representative end member isotopic compositions and by solving the two-component mixing model. The results suggest varying contribution of advected westerly component with an increasing trend up to 65°S. Beyond 65°S, the proportion of Antarctic moisture was found to be prominent and increasing linearly towards the coast.

1 Introduction

The knowledge of factors governing the evaporation of water from the oceans is an essential part of our understanding of the hydrological cycle. The oceans regulate the climate of the earth through heat and moisture transport (Chahine, 1992). Nearly $\approx$ 97% of the water of earth is in the oceans as saline while the residual $\approx$ 3% is fresh water stored in groundwater, glaciers and lakes, or flowing as rivers and streams (Korzoun and Sokolov, 1978). Evaporation of ocean water generates vapour and forms the initial reservoir for circulation in the hydrological cycle. A fraction of this vapor, only $\approx$ 10% of it is transported inland to generate precipitation, while rest of the moisture precipitates over the ocean during its transit (Oki and Kanae, 2006; Shiklomanov, 1998).

Measurements of the isotope composition of water in the various reservoirs of the hydrological cycle operating over the oceans is useful to infer information about the origin of water masses and understanding the formation mechanisms, transport pathways and finally the precipitation processes (Craig, 1961; Dansgaard, 1964; Yoshimura, 2015; Gat, 1996; Araguás-Araguás et al., 2000; Noone and Sturm, 2010; Gat et al., 2003; Benetti et al., 2014; Galewsky et al., 2016). Comparatively large volume of data exists over land to understand the terrestrial hydrological cycle, through the Global Network in Precipitation (GNIP) initiative of the International Atomic Energy Agency (IAEA). However, only a handful records on the spatial and temporal variability of precipitation and vapor isotopic composition over the oceans is available for any assessment (e.g. the Indian Ocean and the Southern Ocean (Uemura et al., 2008; Rahul et al., 2018; Prasanna et al., 2018), the Atlantic Ocean (Benetti et al., 2017b, a, 2015) and Mediterranean Sea (Gat et al., 2003)). Hence further effort is needed to enhance the spatial and temporal sampling coverage over the oceans.

The isotopic composition of vapor on top of a water body is governed by the factors: i) Thermodynamic equilibrium process for phase transformation at a particular temperature ii) Kinetic or non-equilibrium processes where role of relative humidity and wind is significant and iii) Large-scale transport and mixing: due to the movement of air parcels laterally and vertically. Craig and Gordon (1965) initially proposed a two-layer model to simulate the isotopic composition of evaporated (referred to as the Traditional Craig-Gordon model). Recently, Gonfiantini et al. (2018) put forward a modified version referred to as the Unified Craig-Gordon Model. Both of these models incorporate the equilibrium and kinetic processes to simulate the isotopic composition of evaporated moisture. However, in order to get a realistic picture of the hydrological cycle over the ocean, the horizontal transport/advective mixing is important and should be incorporated.

In this paper we present stable isotope ratios in water vapor and ocean surface water from different locations covering varied oceanic settings; i.e. tropical, subtropical and polar latitudes, with a large range in the sea surface temperature, relative humidity and wind speed. While the role of temperature dependent equilibrium fractionation is well understood, the role of kinetic processes is under debate and requires further scrutiny. The performance of these Craig-Gordon evaporation models to simulate the isotopic composition of evaporation flux is evaluated along the sampling transect for different molecular diffusivity ratios and different fractions of molecular vs turbulent diffusion. The models and the conditions that best match with the observations are identified, which are then used to calculate the local evaporation flux. This as done in the context of estimating the contribution of advected vs in-situ derived vapor along the sampling transect assuming a complete mixing of the advected and the locally generated vapor in the sampled water vapor in our study.

2 Methods

2.1 Sampling, isotopic analysis and meteorological parameters

The samples (water vapor, and surface water) for this study were collected along the stretch from Mauritius to Prydz Bay (24°S to 69°S and 57°E to 76°E) during two successive austral summers (January 2017 (SOE-IX) and December 2017 to January 2018 (SOE-X)) onboard the ocean research vessel SA Agulhas. The water vapor sampling inlet was set at $\approx$ 15m above the sea level. An aggregate of 71 water vapor samples were collected during the two expeditions. Fig. 1 shows the water vapor sampling

locations. Alongside water vapor, 49 surface water samples were also collected. The details about the sampling procedures for collection of water vapor and surface water samples are given in the supplementary document. All these subjected to isotopic analysis using Finnigan Gasbench peripheral connected with an isotope ratio mass spectrometer (ThermoScientific MAT 253) (details are provided in the supplementary document). The isotope ratios are expressed in ‰ using the standard δ notation relative to Vienna Standard Mean Ocean Water (VSMOW).

Along with water samples, relative humidity (h), wind speed (ws), air temperature (Ta), sea surface temperature (sst), and atmospheric pressure (P) was recorded continuously during the expedition. Fig. 2 shows the latitudinal variation of these meteorological parameters. A wide range of these physical conditions are encountered since the sampling encompasses a large latitudinal transect.

2.2 Backward air-mass trajectories

In order to reconstruct the vertical profile of the atmospheric moisture transport along the sampling transect, backward air mass trajectories were generated using the Hybrid Single Particle Lagrangian Integrated Trajectory (HYSPLIT) model (Draxler and Hess, 1998; Stein et al., 2015) of NOAA-NCEP/NCAR forced with the Reanalysis data (Kanamitsu et al., 2002). HYSPLIT is a computational model hybrid between Lagrangian and Eulerian methods which generates the paths traversed by the air parcels and calculates meteorological variables such as temperature, relative humidity, specific humidity, rainfall, pressure etc. along the route. Back trajectories for 3 days are extracted since the average residence time of atmospheric moisture over the oceans is ≈3 days Trenberth (1998); Van Der Ent and Tuinenburg (2017). Figure 3 shows the back trajectories for the water vapor sampling locations. The sampling locations can be broadly categorized into zones which are defined by different wind patterns (i.e. velocity and the moisture carrying capacity). Westerlies and polar easterlies were identified based these 72 hour back-trajectories constructed at three different heights above the ocean surface. During the SOE X expedition, the change in trajectories to westerlies was at ≈31°S. At ≈63°S, change from westerlies to polar easterlies is seen. For SOE IX the transition from the westerlies to easterlies and then to polar westerlies was documented at the ≈33°S and ≈64°S latitudes respectively.

2.3 The Craig-Gordon Models

Craig-Gordon in 1965 (CG) Craig and Gordon (1965) proposed the first theoretical model to explain the isotopic composition of water vapor during the evaporation process. The isotopic composition of vapor generated on top of the ocean water depends on the isotopic composition of the surface oceanic water, the isotopic composition of water vapor in the ambient atmosphere along with the relative humidity at the site of sample collection. The interplay of equilibrium and kinetic fractionation between these phases governs the final isotopic composition in the water vapour and liquid. The equilibrium fractionation between ocean water and vapor is controlled by the sea surface temperature (sst). In comparison, relative humidity and wind speed control the the kinetic fractionation through the combination of processes which include both molecular and turbulent diffusion. Molecular diffusion leads to isotopic fractionation between liquid and vapor whereas the turbulent diffusion is non-fractionating. To estimate the isotopic composition of water vapor CG model invokes two-layers; a laminar layer above the air-water interface where the transport process is active via molecular diffusion and a turbulent layer above the laminar layer in which the molecu-

lar transfer is predominantly by the action of turbulent diffusion. Assuming there is no divergence/convergence of air mass over the oceanic atmosphere, the isotopic ratio of the evaporation flux is given as Craig and Gordon (1965) referred to as Traditional Craig-Gordon Model (TCG):

$$R_{ev} = \alpha_k . \frac{R_L . \alpha_{eq} - h . R_A}{1 - h} \tag{1}$$

Where R_L, R_A, h, α_k and α_{eq} are respectively, the isotopic composition of the liquid water, the isotopic composition environmental atmospheric moisture, relative humidity, the kinetic and the equilibrium fractionation factors. The TCG models in this form and with modifications have been used in diverse applications numerous studies studies. Above the ocean one can assume that a steady state is achieved in which the isotopic composition of vapor removed from the system has the same composition as atmospheric vapor (Merlivat, 1978). This is the global closure assumption, i.e,

$$R_A = R_{ev} \tag{2}$$

the global closure assumption (Eq. 2), is substituted in Eq (1) to give;

$$R_{ev} = \alpha_k . \frac{R_L . \alpha_{eq} - h . R_{ev}}{1 - h} \tag{3}$$

$$R_{ev}(1 - h) = \alpha_k . [R_L . \alpha_{eq} - h . R_{ev}] \tag{4}$$

$$R_{ev}(1 - h) + \alpha_k h . R_{ev} = \alpha_k . R_L . \alpha_{eq} \tag{5}$$

$$R_{ev}[(1 - h) + \alpha_k . h] = \alpha_k . R_L . \alpha_{eq} \tag{6}$$

$$R_{ev} = \frac{\alpha_{eq} \alpha_k R_L}{(1 - h) + \alpha_k . h} \tag{7}$$

Recently, Gonfiantini et al. (2018) proposed a modified version of the model, termed as Unified Craig-Gordon (UCG) model in which the parameters controlling the isotopic composition of the evaporation flux are considered simultaneously. From Gonfiantini et al. (2018), the net evaporation rate of liquid water (E) is the difference between the vaporization rate, ψ_{vap}, and the atmospheric vapor capture rate (i.e; condensation) by the liquid water, ψ_{cap}.

$$E = \psi_{vap} - \psi_{cap} = (\gamma - h)\psi^{o}_{cap} \tag{8}$$

Where the ψ^o_{cap} is the vaporization rate of pure water, h is the relative humidity and γ is the thermodynamic activity coefficient of evaporating water which is <1 for the saline solutions and 1 for the pure water or dilute solutions.

From eq. (8), We can write;

$$R_{ev}(\gamma - h)\Psi^o_{vap} = R_{esc}\gamma\Psi^o_{vap} - R_{cap}h\Psi^o_{vap} \tag{9}$$

$$R_{ev}(\gamma - h)\Psi^o_{vap} = \frac{R_L}{\alpha_{eq}\alpha^x_{diff}}\gamma\Psi^o_{vap} - \frac{R_A}{\alpha^x_{diff}}h\Psi^o_{vap} \tag{10}$$

$$R_{ev} = \frac{\frac{R_L}{\alpha_{eq}\alpha^x_{diff}}\gamma - \frac{R_A}{\alpha^x_{diff}}h}{\gamma - h} \tag{11}$$

Where R_L, R_{esc}, R_{cap} and R_A are, respectively the isotopic composition of the liquid water, isotopic composition of vapor escaping to the saturated layer above which is in thermodynamic equilibrium with water, isotopic composition of environmental atmospheric moisture captured by the equilibrium layer and the isotopic composition environmental atmospheric moisture. R_L, R_{esc}, R_{cap} and R_A are defined as in Gonfiantini et al. (2018). α_{eq} is the isotopic fractionation factor between the liquid water and the vapor in the equilibrium layer. α_{diff} is the isotopic fractionation factor for diffusion in air affecting the vapor escaping from the equilibrium layer and the environmental vapor entering the equilibrium layer; x is the turbulent index of atmosphere. Introducing the global closure assumption, Eq. (2) in (11) gives;

$$R_{ev} = \frac{\frac{R_L}{\alpha_{eq}\alpha^x_{diff}}\gamma - \frac{R_{ev}}{\alpha^x_{diff}}h}{\gamma - h} \tag{12}$$

$$R_{ev}(\gamma - h) = \frac{R_L}{\alpha_{eq}\alpha^x_{diff}}\gamma - \frac{R_{ev}}{\alpha^x_{diff}}h \tag{13}$$

$$R_{ev}(\gamma - h) + \frac{R_{ev}}{\alpha^x_{diff}}h = \frac{R_L}{\alpha_{eq}\alpha^x_{diff}}\gamma \tag{14}$$

$$R_{ev}[(\gamma - h) + \frac{h}{\alpha^x_{diff}}] = \frac{R_L}{\alpha_{eq}\alpha^x_{diff}}\gamma \tag{15}$$

$$R_{ev}[\frac{(\gamma - h)\alpha^x_{diff} + h}{\alpha^x_{diff}}] = \frac{R_L}{\alpha_{eq}\alpha^x_{diff}}\gamma \tag{16}$$

$$R_{ev} = \frac{R_L}{\alpha_{eq}\alpha^x_{diff}}\gamma[\frac{\alpha^x_{diff}}{(\gamma - h)\alpha^x_{diff} + h}] \tag{17}$$

$$R_{ev} = \frac{R_L \gamma}{\alpha_{eq}[\alpha^x_{diff}(\gamma - h) + h]} \quad (18)$$

The temperature dependent equilibrium fractionation factor is calculated using the formulation given by (Horita and Wesolowski, 1994). The kinetic factor takes into account diffusion in air affecting the vapor escaping from the equilibrium layer and is controlled by α_{diff}, which is the molecular diffusivity of the different isotopologues of water. Molecular diffusivities ($H_2^{18}O/H_2^{16}O$, $H^2H^{16}O/H_2^{16}O$) data are taken from three previous studies Merlivat (1978) (1.0285, 1.0251), Cappa et al. (2003) (1.0318, 1.0164) and Pfahl and Wernli (2009) (1.0076, 1.0039) referred to as MJ, CD and PW respectively. x is the turbulence index of atmosphere. When x = 1 the vapor escapes solely by molecular diffusion and for x = 0 the vapor escapes only due to turbulent diffusion.

3 Results

3.1 Isotopic measurements along the transect

$\delta^{18}O$ of surface water was > 0 ‰ until ≈ 40°S latitude. A transition to lighter isotopic composition was observed beyond ≈ 45°S latitude with a drop documented in the surface water isotopic values on approaching the coastal Antarctic regions. Figure 4a shows the latitudinal variation of $\delta^{18}O_{sw}$, plotted along with salinity values measured along the transect. In addition, the $\delta^{18}O$ of ocean surface water extracted from the Global Sea Water 18O Database (SWD) (Schmidt et al., 1999) are also plotted. There is a mismatch between the observed depleted isotopic values near coastal Antarctica with SWD values. The SWD is a surface interpolated dataset based on point observations in the global ocean. This is probably one of the major causes of the difference, the others being the season or the month of sample collection.

The $\delta^{18}O_{wv}$ and δ^2H_{wv} in water vapor samples showed a consistent trend across latitude for both the expeditions. The $\delta^{18}O_{wv}$ (δ^2H_{wv}) of water vapor varies from -10.9‰ (-80.8‰) to -27.5‰(-221.4‰) respectively. The vapor isotopic composition is seen to be gradually decreasing with lighter isotopic values at higher latitudes. A steady drop was noted from ≈30°S to ≈65°S and a sharp change in the gradient was registered at ≈65°S. Extreme lighter values were recorded on approaching ≈65°S are attributed to factors like low temperature and the mixing of lighter vapor from continental Antarctica (Uemura et al., 2008). There are deviations from this general trend with heavier isotopic composition observed at the higher latitudes or vice versa. These variations can be accounted, by taking into consideration the source and the path of air masses. The lighter (heavier) values of vapor isotopic composition can be traced to the source being lower (higher) latitudes.

Deuterium excess (d-excess or dxs), defined as $d - excess = \delta^2H - 8 \times \delta^{18}O$, is a second order isotope parameter which is a measure of kinetic fractionation during evaporation (Dansgaard, 1964). d-excess in the water vapor correlates with meteorological parameters at the ocean surface such as relative humidity, sea surface temperature and wind speed (Uemura et al., 2008; Rahul et al., 2018; Benetti et al., 2014; Midhun et al., 2013). Therefore, it serves as a proxy for the moisture source conditions in the evaporation regions. The dxs and relative humidity are strongly coupled, which is determined by the magnitude of moisture gradient between evaporating water surface and overlying unsaturated air. In other words, lower the relative humidity

higher is the dxs in the overlying moisture. Wind speed regulates the turbulent vs molecular diffusion across the diffusive layer. The role of sst in governing the dxs is through the process of equilibrium fractionation, which is temperature dependent. The dxs values in water vapor samples range from 18.7‰ to -23.7‰. A relatively higher dxs values in the water vapor from ≈25°S to ≈45°S with a slight step change to lower dxs values was recorded on approaching 45°S which extends until ≈65°S. Beyond ≈ 65°S a slight increment in the vapor dxs was observed as depicted in the box-plot in Figure 4d. The very low dxs values, caused due to mixing of vapor evaporated from sea-spray under high wind speed conditions are observed during the passage of extra-tropical cyclones. The statistics of the isotopic composition of water vapor are tabulated in Table 1.

3.2 Meteorological controls on the isotopic composition of water vapor

The $\delta^{18}O_{wv}$ and $\delta^{2}H_{wv}$ are positively correlated with sst, negatively correlated with wind speed and uncorrelated with relative humidity. For all the water vapor samples, $\delta^{2}H_{wv}$ and $\delta^{18}O_{wv}$ are correlated with sst explaining ≈33% of the variance in $\delta^{18}O_{wv}$ and ≈50% of the variance in $\delta^{2}H_{wv}$. The correlation coefficient is higher if sampling from individual years is considered separately. In all cases, the slope and intercept of the regression equation between the isotopic composition of water vapor and sst is comparable with previous observations from the Southern Ocean Uemura et al. (2008). The linear regression plots are shown Figure 5 and the regression parameters (slope, intercept, standard errors and r^2) for $\delta^{18}O$ and $\delta^{2}H$ are listed in Table 1.(S) and Table 2.(S) respectively. The regression equations are calculated for different sample classifications, with and without the influence of Antarctic vapor mixing as evident from the back trajectories (i.e. samples collected north of 65°S) and for individual expeditions.

Figure 6 shows the regression plots of dxs in vapor with the meteorological conditions and the parameters defining the regression equations are listed in Table 2. For samples collected north of 65°S, the linear regression equation describing the relationship between dxs and relative humidity is dxs=-0.56h+46.36 (r^2=0.49). These slope and intercept values are similar to the earlier records, documenting the isotope variability in water vapour from the Southern Ocean (Uemura et al., 2008; Rahul et al., 2018) the Bay of Bengal (Midhun et al., 2013), the Atlantic (Benetti et al., 2014) and the Mediterranean (Gat et al., 2003). For samples collected south of 65°S the relationship becomes weaker. The strength of the dxs vs h relationship was stronger if data exclusively from the expeditions is considered separately, for the SOE IX and SOE X as dxs=-0.64h+57.4 (r^2=0.77) and dxs=-0.64h+48.7 (r^2=0.61) respectively. Collectively for both the expeditions, the dxs in vapor is positively correlated with the sst and the regression parameters are comparable with those from previous observations in the Southern Ocean and also for the Atlantic Ocean and the Bay of Bengal. For sst vs dxs, the linear regression equation for samples collected north of 65°S is given by dxs=0.70sst-4.65 (r^2=0.49). The dxs of water vapor samples are negatively correlated with wind speed. For samples collected north of 65°S the correlation the regression equation is given by dxs=-0.53ws+11.65 (r^2=0.23). Our observation is consistent with the earlier studies suggesting the dependency of water vapor d-excess on relative humidity, sst and wind speed.

4 Discussion

4.1 Craig-Gordon (CG) model evaluation

The isotopic composition of evaporation flux from the oceans is calculated using the CG models (TCG and UCG) assuming three molecular diffusivity ratios driving the kinetic fractionation and for varied contribution of turbulent vs molecular diffusion enabled transport factors. The simulated values of the isotopic composition of evaporation flux with these different models are compared with the measured isotopic values of water vapor over the ocean. The model and the constraints than best describes the observations are selected based on the model predicted and observed relationships between the dxs of water vapor and physical parameters (sst, ws and rh).

The TCG and the UCG models are run for MJ, CD and PW molecular diffusivities and for the turbulence index of the atmosphere varying from 0-1 with an increment of 0.1. Figure 7 and Figure 8 shows the comparison between the TCG and UCG modelled vapor isotopic composition ($\delta^{18}O$ and d-excess) with the observations. There are values for the turbulence index (x) of the atmosphere where model predicted $\delta^{18}O$ and d-excess overlap with the observations for both TCG and UCG models with MJ and CD molecular diffusivity ratios. However, there is a clear mismatch between the model predicted $\delta^{18}O$ and d-excess for the recommended PW molecular diffusivities in both UCG and TCG models. Another noteworthy feature of the plots is the for all the model runs a large difference is seen between the modelled and observed isotopic composition for water vapor samples collected south of $\approx 65°$S latitudes and the best match is seen for samples collected North of $\approx 65°$S. This difference is attributed to the advection and mixing of lighter Antarctic moisture to local moisture for samples collected beyond $\approx 65°$S.

To evaluate the performance of the prediction by these models and identify the parameters that best describe the observations, the slope of the dxs vs relative humidity predicted by the different model runs are compared with the observed relationships documented based on actual data on samples collected north of 65°S. Figure 1.(S) depicts the comparison between the observed and the model predicted relationships. The UCG models and the parameters that match the observed slope of the relative humidity vs d-excess relationship (-0.56 ± 0.08) are $UCG^{MJ}_{x=0.8}$, $UCG^{CD}_{x=0.6}$ and $UCG^{PW}_{x=0}$. Similarly for the TCG models $TCG^{MJ}_{x=0.6}$, $TCG^{CD}_{x=0.7}$ and $TCG^{PW}_{x=0}$ predict the slopes that are comparable with the observed value. The $\delta^{18}O$ d-excess of predicted by these models are plotted with the observations in Figure 9.

The consistency of model results and observation are best described using a linear regression equation which link model predicted d-excess and the meteorological parameters (relative humidity, sea surface temperature and wind speed). These regression plots are displayed in Figure 2.(S). The difference between the model predicted and the observed values of slopes and intercepts are shown in Figure 10. The largest difference between the observed and model predicted slopes are intercepts are for the PW molecular diffusivities for both UCG and the TCG models and therefore excluded from further discussion. For the dxs vs relative humidity relationship, $UCG^{MJ}_{x=0.8}$ and $UCG^{CD}_{x=0.6}$ show the smallest difference between the observed and modelled slopes and intercepts followed by $TCG^{MJ}_{x=0.6}$ and $TCG^{CD}_{x=0.7}$. In case of dxs vs sst relationship,'the TCG models show the least difference between the slopes and the UCG model predicts the intercept values that are consistent with the observations. Similarly, for the and dxs vs ws relationships, the UCG and the TCG models produce the values that are predict

the slope and the intercept values with the least deviation from the observed values. The models that best describe the slope and intercept values of linear regression equation defining the d-excess vs the meteorological parameters, the root mean square error of the modelled vs observed $\delta^{18}O$ and d-excess are listed in Table 3. The ability of the models to predict the $\delta^{18}O$ and d-excess are better demonstrated by the water vapor samples which were collected north of 65°S are considered. The models predict the d-excess with a better correlation than $\delta^{18}O$ and the TCG model show a slightly higher possibility to predict the d-excess values than the UCG model.

4.2 Understanding the equilibrium/disequilibrium

The isotopic composition of water vapor over the ocean is governed by the equilibrium and kinetic processes which are defined by the meteorological condition. However, considering only these factors insufficient to explain the observed variation in the isotopic composition of vapor on top of the ocean. The process like advective mixing of transported vapor to the locally generated vapor is important and needs to be taken into consideration. Fig. 11a shows the difference between the $\delta^{18}O$ and $\delta^{2}H$ isotopic composition of vapor (at equilibrium with ocean surface water) and the observed vapor isotopic composition. Kinetic fractionation can explain a part of the departure from the equilibrium state and is evaluated based on the Craig-Gordon models as described in the previous section ($E_{UCG}^{MJ,0.8}$, $E_{UCG}^{CD,0.6}$, $E_{TCG}^{MJ,0.6}$ and $E_{TCG}^{CD,0.7}$). The difference between isotopic composition of equilibrium vapor ($\delta^{18}O$ and $\delta^{2}H$) and the modelled isotopic composition by the E_{UCG}, E_{TCG} is also plotted in Figure 11b-e. In order to calculate the fractional contribution of the local and advected moisture along the sampling transect, a two component mixing framework is invoked. The local end member is based on the isotopic composition of vapor predicted by the best match UCG and the TCG model predicted parameters. The calculations are done assuming the isotopic composition of the advected vapor due to westerlies similar to the earlier proposition (Uemura et al., 2008) ($\delta^{2}H \approx$-109‰) in the region between 31°S to 65°S. For samples collected in the polar ocean south of 65°S, the temperature plays the role of limiting the local evaporation process and hence the large differences from the equilibrium conditions can be explained by invoking the process of mixing of Antarctic vapor which is transported to this region by the interplay of polar easterlies. The average isotopic composition of water vapor collected at Dome C site (Dec 2014-Jan) (Wei et al., 2019) ($\delta^{2}H$= -490±23‰) is chosen as representative of the advected vapor transported by the polar easterlies. It is seen that in order to explain the water vapor isotope ratio observation over the ocean south of 65°S, the contribution of lighter Antarctic vapor is expected. Fig. 12b shows the relative contribution of advected and locally generated moisture in our observation. The advected component is a prominent component of the ambient vapor on approaching higher latitudes. South of 65°S the amount of moisture present in the atmosphere is less and is largely local in origin with a small mixing of lighter Antarctic vapor. However, the contribution of which linearly increases on approaching the coastal regions.

5 Conclusions

In this study, the isotopic composition of water vapor and surface water samples collected across a latitudinal transect from Mauritius to Prydz in the Southern Ocean are described. The isotopic composition of evaporating vapor is governed by the iso-

topic composition of the water, ambient vapor isotopic composition, exchange and mixing processes at the water-air interface as well as the local meteorological conditions. These controlling parameters were considered separately or simultaneously for explaining the observation best quantifying the evaporation mechanism adopted in the Craig-Gordon models. The Traditional (Craig and Gordon, 1965) (TCG) and the Unified C-G (UCG) (Gonfiantini et al., 2018) equations were used to predict the isotopic composition of evaporation flux after incorporating different molecular diffusivity ratios at varying fractions of molecular and turbulent diffusion. $UCG^{MJ}_{x=0.8}, UCG^{CD}_{x=0.6}, TCG^{MJ}_{x=0.6}$ and $TCG^{CD}_{x=0.7}$ models predicted the slope and the intercepts of dxs vs meteorological parameters with an appreciable accuracy and consistent with the observations. The results ascertain the importance of the fraction of molecular vs turbulent fraction used to predict the isotopic composition of evaporation in the Craig-Gordon models. The relative contribution of advected and evaporated fluxes was estimated by assigning end member isotopic composition and solving in a two-component mixing framework. The approximation of the locally generated end member composition is based on $UCG^{MJ}_{x=0.8}, UCG^{CD}_{x=0.6}, TCG^{MJ}_{x=0.6}$ and $TCG^{CD}_{x=0.7}$. The advected moisture flux is assigned values based on the origin and path followed by the back trajectories. It is found that beyond 65S latitude lighter isotope values observed in the water can be explained by invoking mixing of Antarctic vapor with linearly increasing contribution towards the coast.

Author contributions

SSD and PG conceptualized the study. SSD and AS performed the sample collection and analysis. SSD wrote the paper and PG supervised the study. AK provided the resources during the expeditions.

Acknowledgements

We would like to thank the Ministry of Earth Sciences, Government of India, the National Centre for Polar and Ocean Research, Goa, India and members of the Scientific Southern Ocean Expeditions.

Data Availability

The data that support the findings of this study have been uploaded as a supplementary document.

Declaration of interests

The authors declare that they have no known competing financial interests or personal relationships that could have appeared to influence the work reported in this paper.

References

Araguás-Araguás, L., Froehlich, K., and Rozanski, K.: Deuterium and oxygen-18 isotope composition of precipitation and atmospheric moisture, Hydrological Processes, 14, 1341–1355, 2000.

Benetti, M., Reverdin, G., Pierre, C., Merlivat, L., Risi, C., Steen-Larsen, H. C., and Vimeux, F.: Deuterium excess in marine water vapor: Dependency on relative humidity and surface wind speed during evaporation, Journal of Geophysical Research: Atmospheres, 119, 584–593, 2014.

Benetti, M., Aloisi, G., Reverdin, G., Risi, C., and Sèze, G.: Importance of boundary layer mixing for the isotopic composition of surface vapor over the subtropical North Atlantic Ocean, Journal of Geophysical Research: Atmospheres, 120, 2190–2209, 2015.

Benetti, M., Reverdin, G., Aloisi, G., and Sveinbjörnsdóttir, Á.: Stable isotopes in surface waters of the Atlantic Ocean: Indicators of ocean-atmosphere water fluxes and oceanic mixing processes, Journal of Geophysical Research: Oceans, 122, 4723–4742, 2017a.

Benetti, M., Steen-Larsen, H. C., Reverdin, G., Sveinbjörnsdóttir, Á. E., Aloisi, G., Berkelhammer, M. B., Bourlès, B., Bourras, D., De Coetlogon, G., Cosgrove, A., et al.: Stable isotopes in the atmospheric marine boundary layer water vapour over the Atlantic Ocean, 2012–2015, Scientific data, 4, 160 128, 2017b.

Cappa, C. D., Hendricks, M. B., DePaolo, D. J., and Cohen, R. C.: Isotopic fractionation of water during evaporation, Journal of Geophysical Research: Atmospheres, 108, 2003.

Chahine, M. T.: The hydrological cycle and its influence on climate, Nature, 359, 373, 1992.

Craig, H.: Isotopic variations in meteoric waters, Science, 133, 1702–1703, 1961.

Craig, H. and Gordon, L. I.: Deuterium and oxygen 18 variations in the ocean and the marine atmosphere, 1965.

Dansgaard, W.: Stable isotopes in precipitation, Tellus, 16, 436–468, 1964.

Draxler, R. R. and Hess, G.: An overview of the HYSPLIT_4 modelling system for trajectories, Australian meteorological magazine, 47, 295–308, 1998.

Galewsky, J., Steen-Larsen, H. C., Field, R. D., Worden, J., Risi, C., and Schneider, M.: Stable isotopes in atmospheric water vapor and applications to the hydrologic cycle, Reviews of Geophysics, 54, 809–865, 2016.

Gat, J., Klein, B., Kushnir, Y., Roether, W., Wernli, H., Yam, R., and Shemesh, A.: Isotope composition of air moisture over the Mediterranean Sea: an index of the air–sea interaction pattern, Tellus B, 55, 953–965, 2003.

Gat, J. R.: Oxygen and hydrogen isotopes in the hydrologic cycle, Annual Review of Earth and Planetary Sciences, 24, 225–262, 1996.

Gonfiantini, R., Wassenaar, L. I., Araguas-Araguas, L., and Aggarwal, P. K.: A unified Craig-Gordon isotope model of stable hydrogen and oxygen isotope fractionation during fresh or saltwater evaporation, Geochimica et Cosmochimica Acta, 235, 224–236, 2018.

Horita, J. and Wesolowski, D. J.: Liquid-vapor fractionation of oxygen and hydrogen isotopes of water from the freezing to the critical temperature, Geochimica et Cosmochimica Acta, 58, 3425–3437, 1994.

Kanamitsu, M., Ebisuzaki, W., Woollen, J., Yang, S.-K., Hnilo, J., Fiorino, M., and Potter, G.: Ncep–doe amip-ii reanalysis (r-2), Bulletin of the American Meteorological Society, 83, 1631–1643, 2002.

Korzoun, V. and Sokolov, A.: World water balance and water resources of the earth, Water Development, Supply and Management (UK)(USA)(Canada)(Australia)(France)(Germany, FR), 1978.

Merlivat, L.: Molecular diffusivities of H 2 16 O, HD 16 O, and H 2 18 O in gases, The Journal of Chemical Physics, 69, 2864–2871, 1978.

Midhun, M., Lekshmy, P., and Ramesh, R.: Hydrogen and oxygen isotopic compositions of water vapor over the Bay of Bengal during monsoon, Geophysical Research Letters, 40, 6324–6328, 2013.

Noone, D. and Sturm, C.: Comprehensive dynamical models of global and regional water isotope distributions, in: Isoscapes, pp. 195–219, Springer, 2010.

Oki, T. and Kanae, S.: Global hydrological cycles and world water resources, science, 313, 1068–1072, 2006.

Pfahl, S. and Wernli, H.: Lagrangian simulations of stable isotopes in water vapor: An evaluation of nonequilibrium fractionation in the Craig-Gordon model, Journal of Geophysical Research: Atmospheres, 114, 2009.

Prasanna, K., Ghosh, P., Bhattacharya, S., Rahul, P., Yoshimura, K., and Anilkumar, N.: Moisture rainout fraction over the Indian Ocean during austral summer based on 18O/16O ratios of surface seawater, rainwater at latitude range of 10 N-60 S., Journal of Earth System Science, 127, 2018.

Rahul, P., Prasanna, K., Ghosh, P., Anilkumar, N., and Yoshimura, K.: Stable isotopes in water vapor and rainwater over Indian sector of Southern Ocean and estimation of fraction of recycled moisture, Scientific reports, 8, 2018.

Schmidt, G., Bigg, G., and Rohling, E.: Global seawater oxygen-18 database–v1. 21, Online at http://data. giss. nasa. gov/o18data, online at http://data. giss. nasa. gov/o18data, 1999.

Shiklomanov, I. A.: World water resources: a new appraisal and assessment for the 21st century: a summary of the monograph World water resources, Unesco, 1998.

Stein, A., Draxler, R., Rolph, G., Stunder, B., Cohen, M., and Ngan, F.: NOAA's HYSPLIT atmospheric transport and dispersion modeling system, Bulletin of the American Meteorological Society, 96, 2059–2077, 2015.

Trenberth, K. E.: Atmospheric moisture residence times and cycling: Implications for rainfall rates and climate change, Climatic change, 39, 667–694, 1998.

Uemura, R., Matsui, Y., Yoshimura, K., Motoyama, H., and Yoshida, N.: Evidence of deuterium excess in water vapor as an indicator of ocean surface conditions, Journal of Geophysical Research: Atmospheres, 113, 2008.

Van Der Ent, R. J. and Tuinenburg, O. A.: The residence time of water in the atmosphere revisited, Hydrology and Earth System Sciences, 21, 779–790, 2017.

Wei, Z., Lee, X., Aemisegger, F., Benetti, M., Berkelhammer, M., Casado, M., Caylor, K., Christner, E., Dyroff, C., García, O., et al.: A global database of water vapor isotopes measured with high temporal resolution infrared laser spectroscopy, Scientific data, 6, 180 302, 2019.

Yoshimura, K.: Stable water isotopes in climatology, meteorology, and hydrology: A review, Journal of the Meteorological Society of Japan. Ser. II, 93, 513–533, 2015.

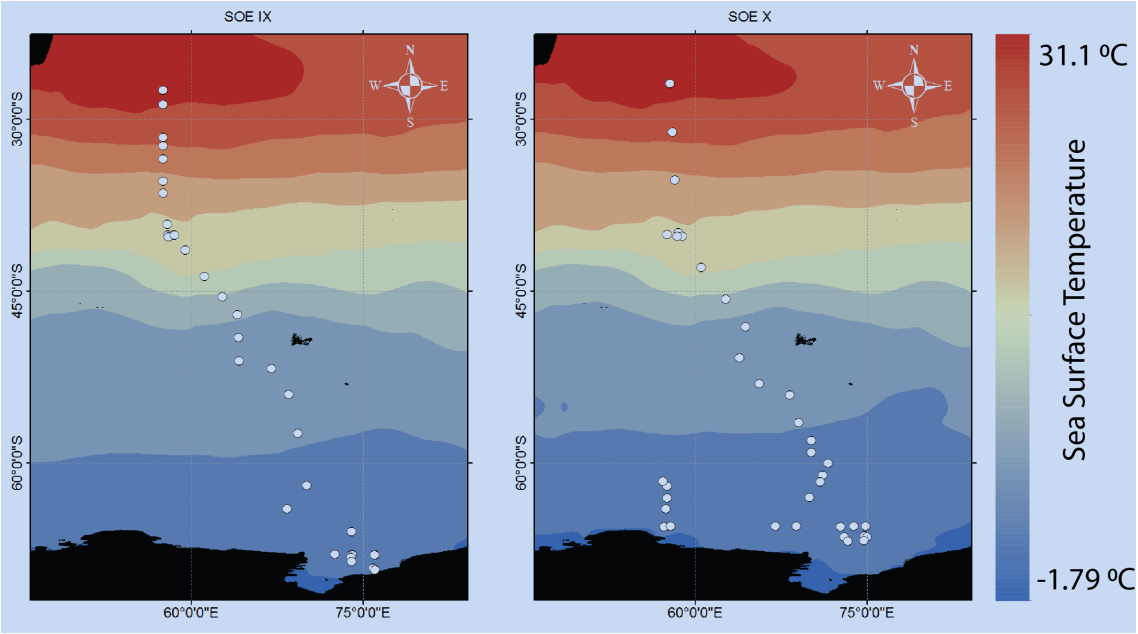

Figure 1. The water vapor sampling location during the two expedition shown as open circles overlain on the map of mean monthly sea surface temperature during the two expeditions. The sea surface temperature data is from Reanalysis dataset Kanamitsu et al. (2002)

Table 1. Descriptive statistics of the water vapor isotopic composition

	$\delta^{18}O(‰)$	$\delta^{2}H(‰)$	**d-excess**(‰)
SOE IX Water Vapor(n=34)			
Max	-10.86	-80.79	18.65
Min	-27.47	-221.38	-8.37
Mean(Stdev)	-16.96(±5.25)	-130.35(±44.43)	5.35(±8.06)
SOE X Water Vapor(n=37)			
Max	-11.46	-88.03	14.54
Min	-21.18	-163.28	-23.71
Mean(Stdev)	-15.77(±2.53)	-126.07(±20.23)	0.08(±8.46)

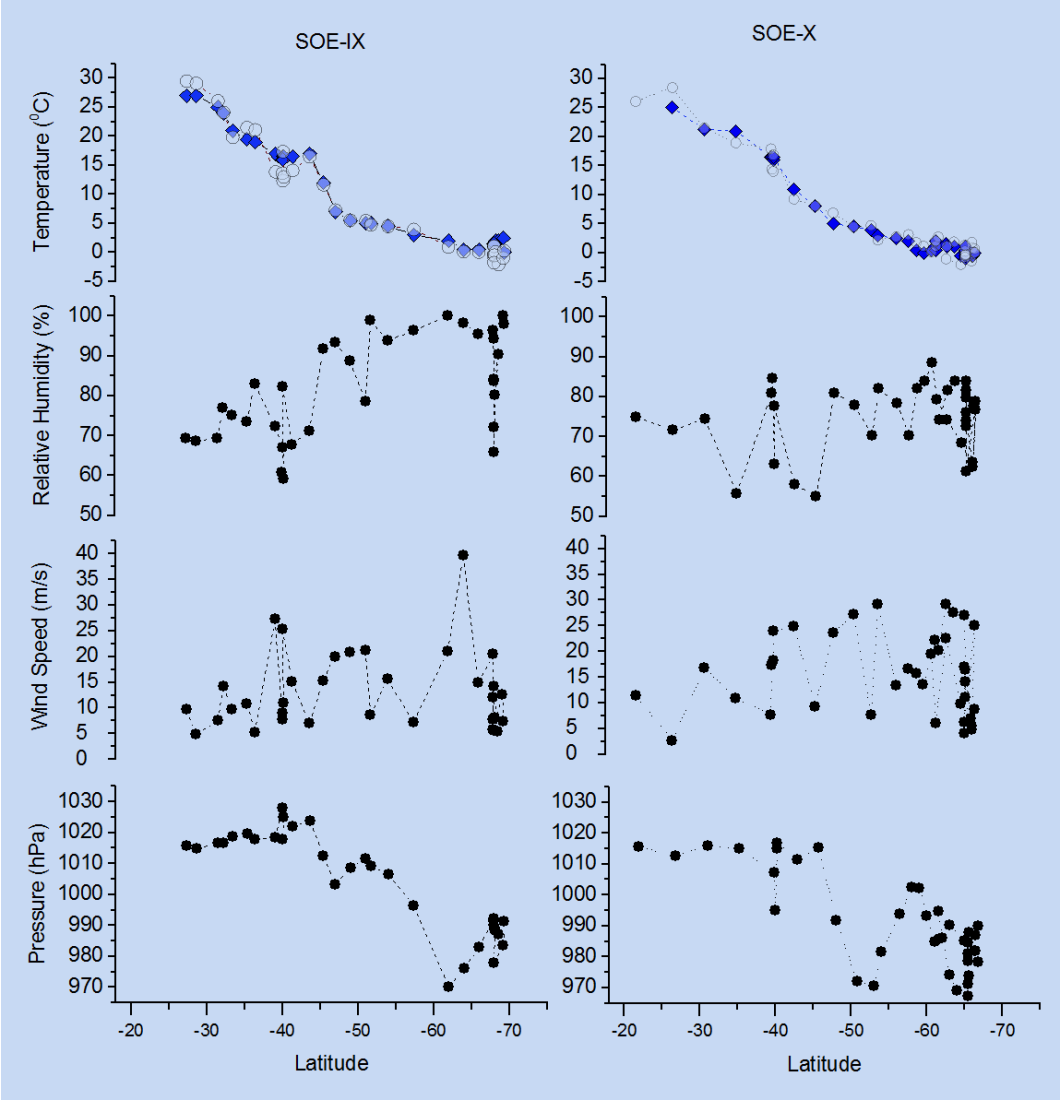

Figure 2. Latitudinal variability of measured meteorological parameters: temperature, relative humidity, wind speed and atmospheric pressure. Filled blue diamonds and open circles in the temperature plot represent the sea surface temperature and air temperature respectively.

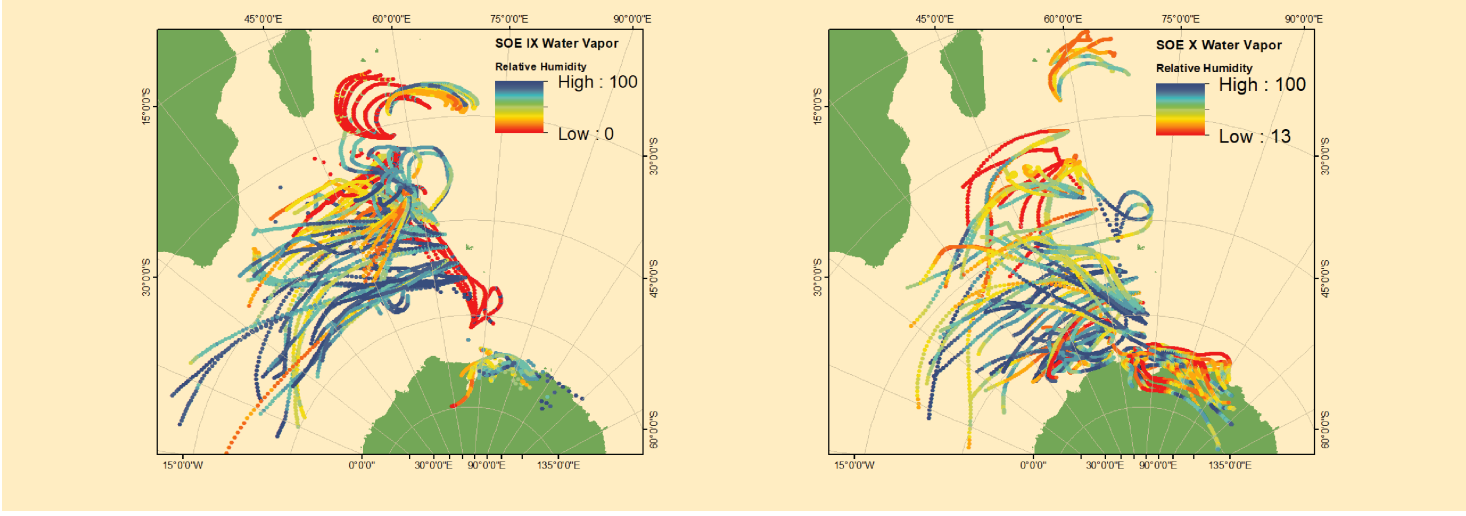

Figure 3. 72 hours back trajectories calculated using HYSPLIT with Reanalysis data as forcing. The trajectories shown are for three heights surface, 500m and 1500m above the mean sea level and the colors depict the variation of relative humidity along the trajectories.

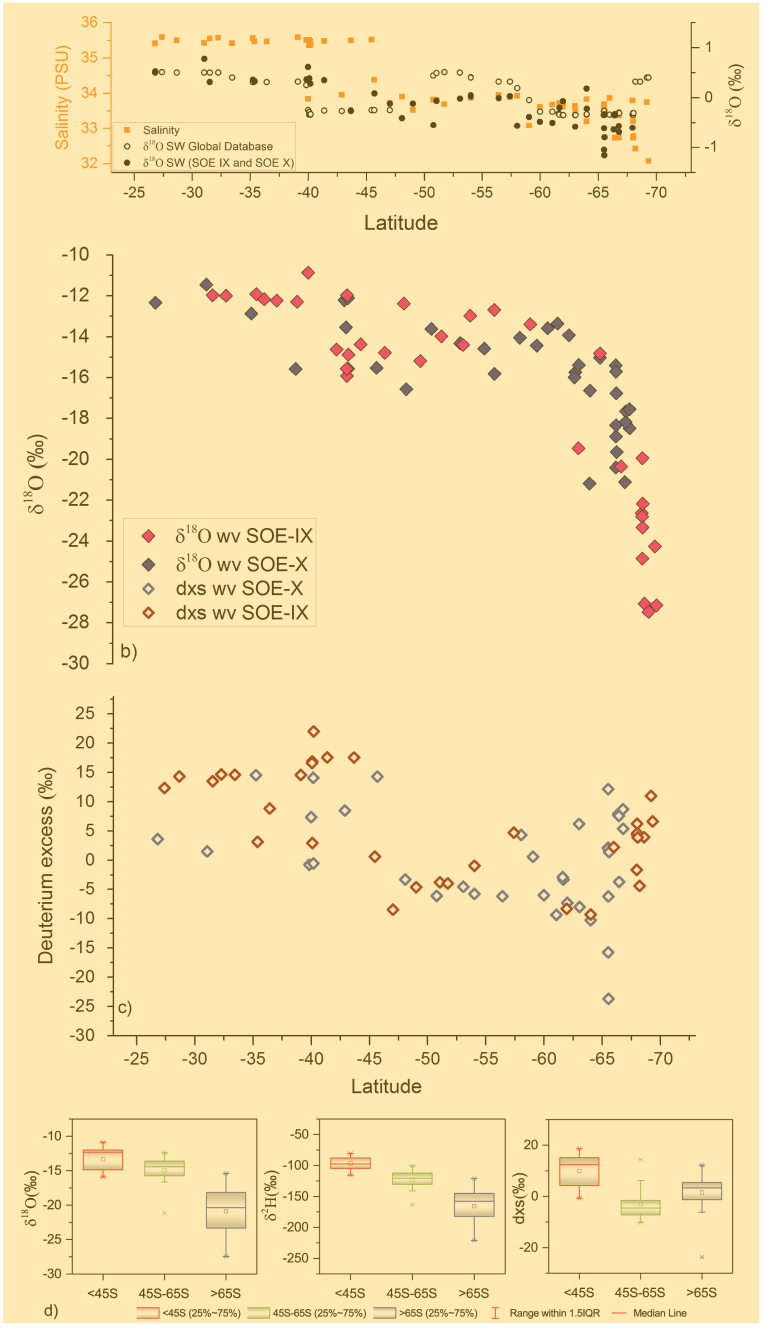

Figure 4. a) Measured $\delta^{18}O_{SW}$ as black filled circled and values of surface water isotopic composition extracted from the global sea water $\delta^{18}O_{SW}$ database along the latitudinal transect (open black circles). Also plotted as orange filled squares are the salinity values along the transect b) Pink and purple filled diamonds depict the $\delta^{18}O_{WV}$ of water vapor samples collected during the SOE-IX and SOE-X respectively at height of $\approx$ 15m above the water surface. c) latitudinal variation of dxs in water vapor samples shown as open red and purple diamonds for SOE-IX and SOE-X respectively, d) variation of $\delta^{18}O$, $\delta^{2}H$ and dxs along the transect as box plots grouped by latitudes based on the HYSPLIT back trajectories.

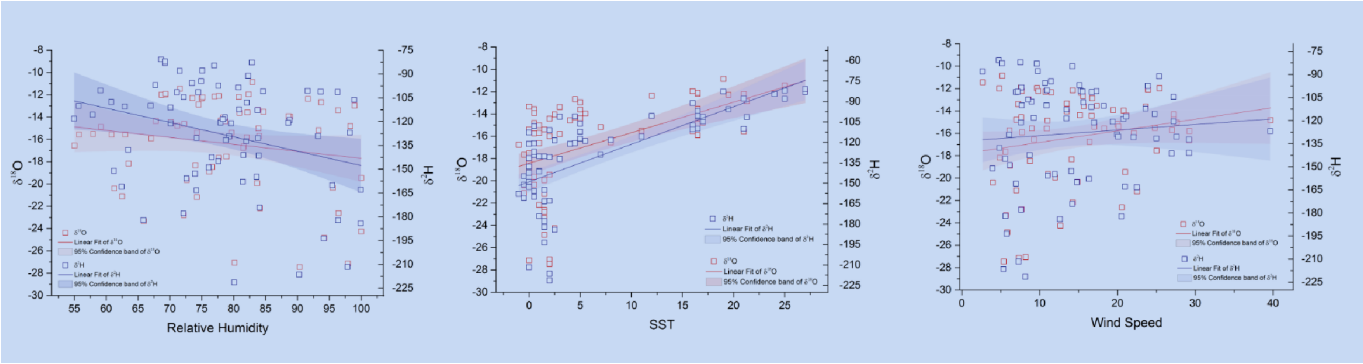

Figure 5. Linear regression for isotopic composition of water vapor and physical parameters(sea surface temperature, relative humidity and wind speed). Hollow red and blue squares represent the $\delta^{18}O$ and $\delta^{2}H$ respectively and the shaded areas depict the 95% confidence bands. The linear regression lines are shown as blue and red for $\delta^{2}H$ and $\delta^{18}O$ respectively. The slope and intercept of the linear regression equations along with data from Uemura et al. (2008) are listed in Table 1.(S) and Table 2 (S)

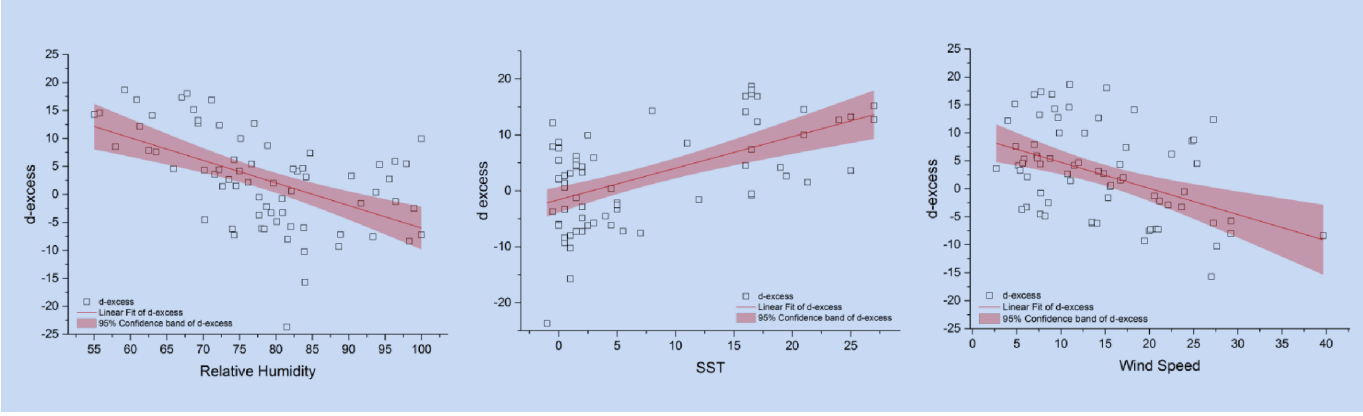

Figure 6. Regression plots for d-excess (hollow black squares) in water vapor and the meteorological conditions (relative humidity, sea surface temperature and wind speed). The shaded region depicts the 95% confidence bands of d-excess. The slope and intercept of the regression equations along with data from Uemura et al. (2008) are listed in Table 2

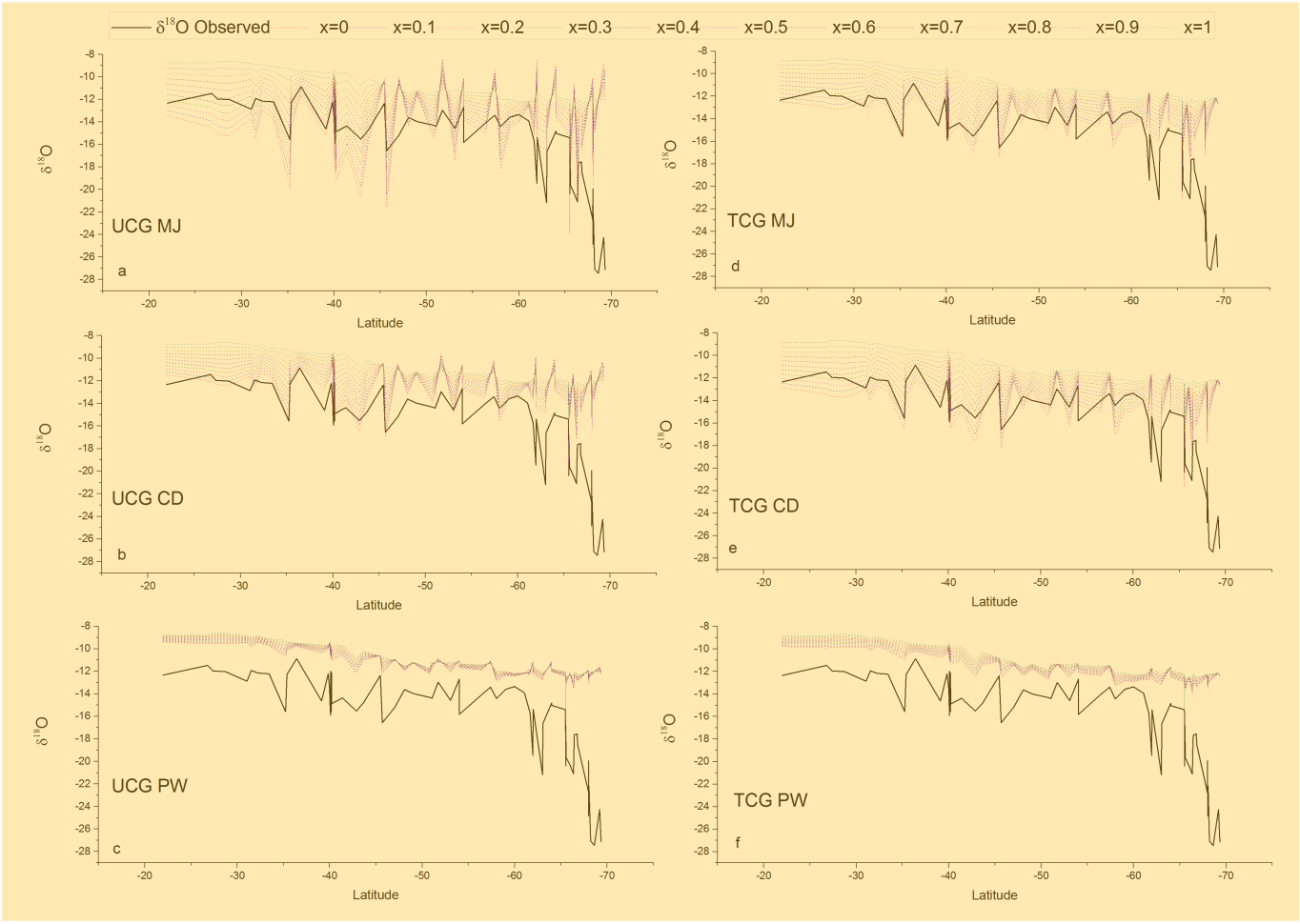

Figure 7. Comparison between the latitudinal distribution of the measured water vapor $\delta^{18}O$ (black lines) and that predicted by the TCG and UCG models for different molecular diffusivity ratios and turbulence indices, shown as colored lines.

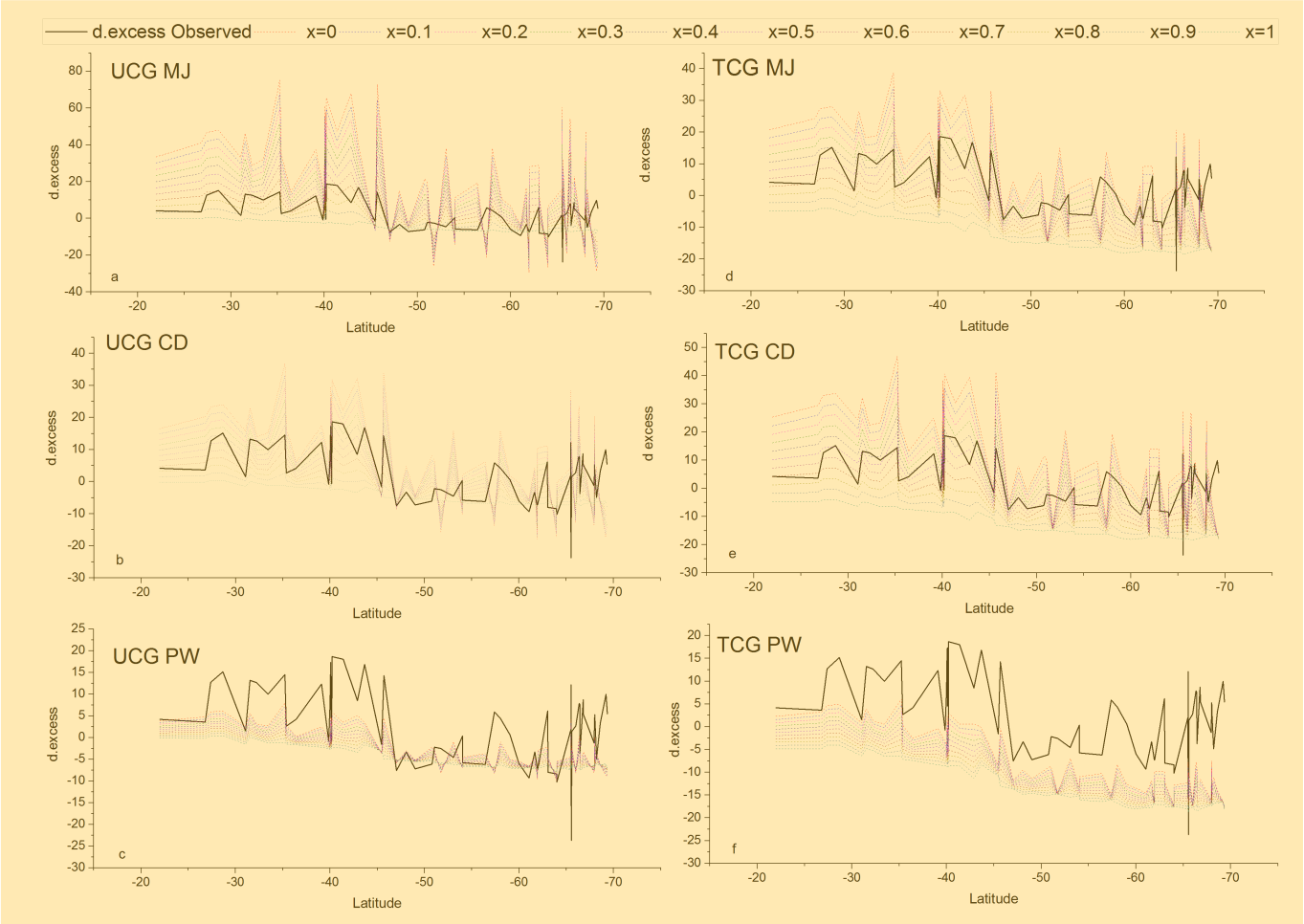

Figure 8. Comparison between the latitudinal distribution of the measured d-excess in water vapor (black lines) and that predicted by the TCG and UCG models for different molecular diffusivity ratios and turbulence indices shown as colored lines

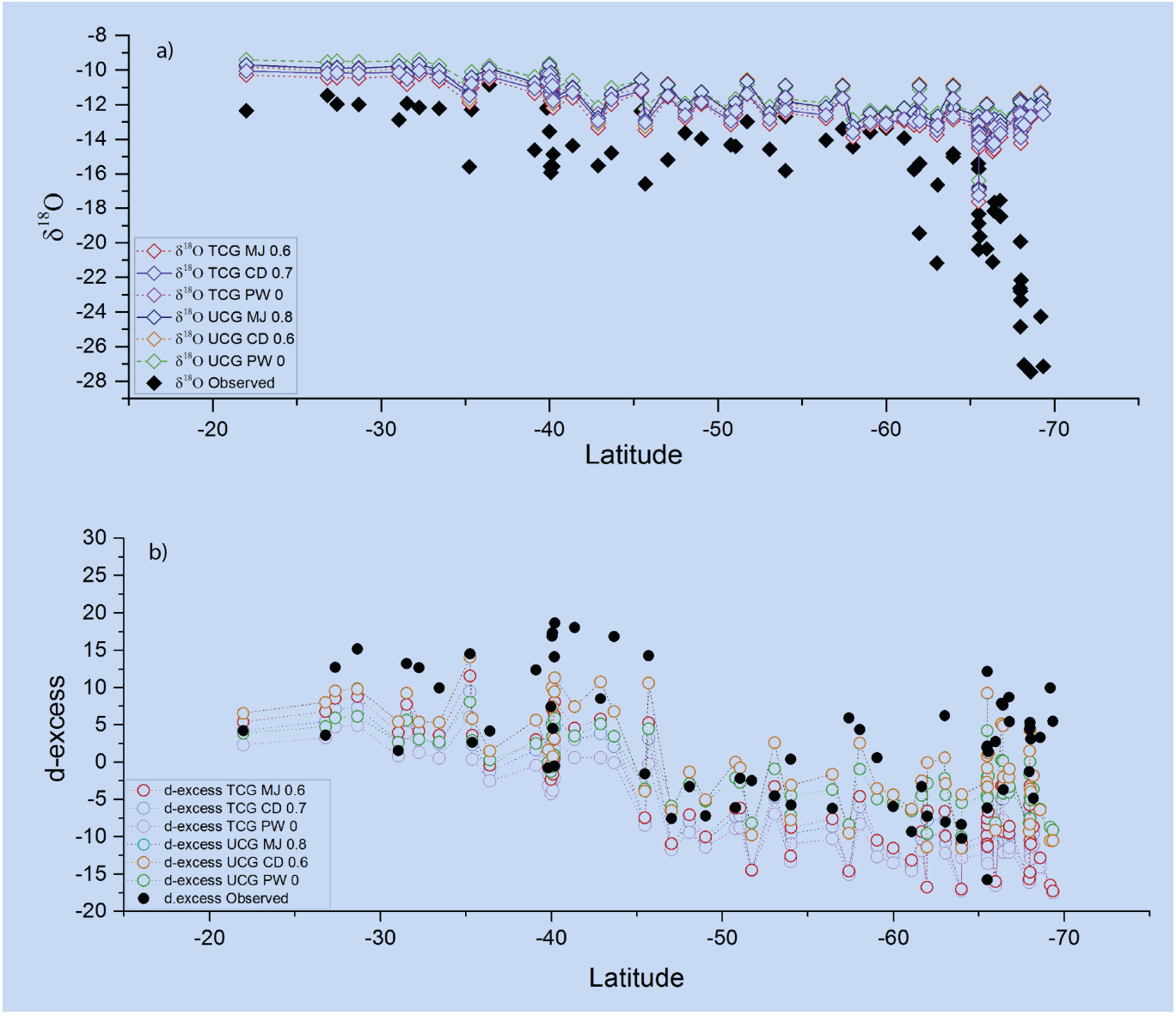

Figure 9. Latitudinal variation of the observed $\delta^{18}O$ (a) as filled black diamonds and d-excess (b) as filled black circles and the modelled values (colored open diamonds and circles) for the model runs where the observed slope is comparable to the modelled slope. The statistical parameters analysis of the observed and modelled regression are listed in Table 3.

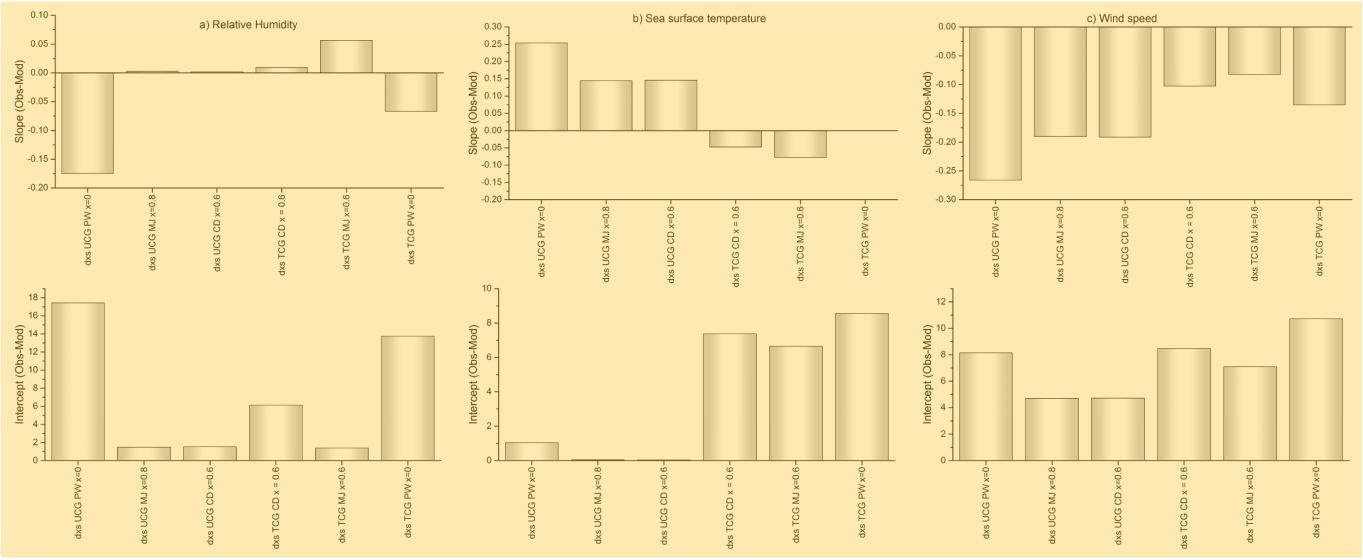

Figure 10. Differences between observed and predicted slopes and intercepts of the relationships between d-excess vs relative humidity, sea surface temperature and wind speed.

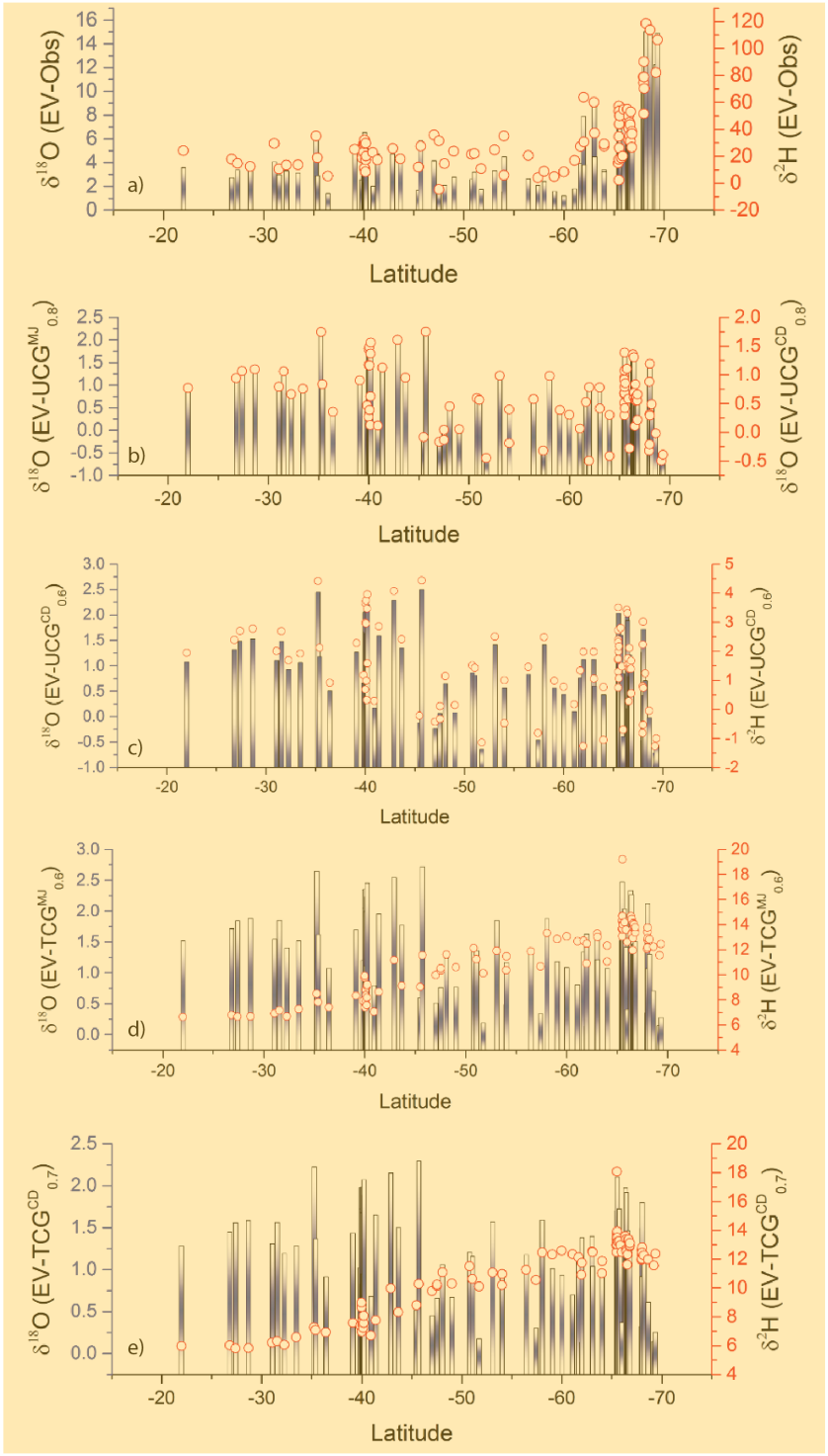

Figure 11. a) the difference between the $\delta^{18}O$ (blue columns) and $\delta^{2}H$ (red open circles) of equilibrium vapor and observed water vapor isotopic composition. b-e) shows difference between the $\delta^{18}O$ and $\delta^{2}H$ equilibrium vapor and that predicted by the best fit model runs.

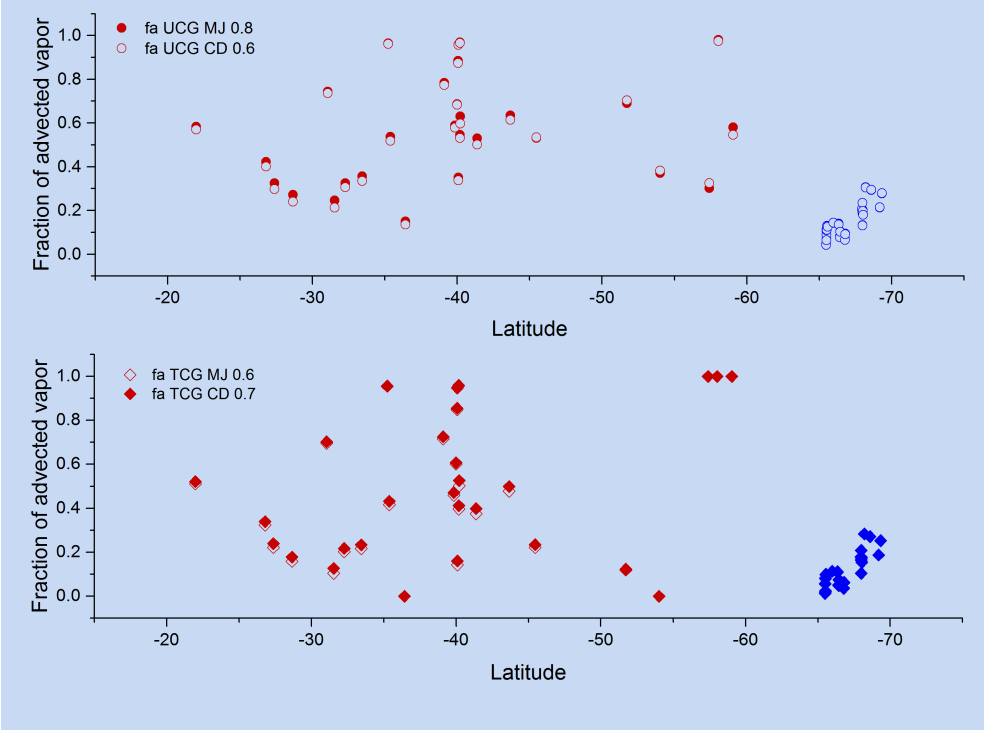

Figure 12. a) Fraction of advected vapor that explains the water vapor isotopic composition for the best fit model runs. Red and blue colors depict the different end member compositions used for calculations.

Table 2. Slope, intercept and r^2 of the linear regression equations between meteorological parameters (relative humidity, sea surface temperature and winds speed) and d-excess for different sample classifications. Also listed are the regression parameters for the data from Uemura et al. (2008)

Met. vs d-excess		Intercept		Slope		Statistics
	Classification	Value	Standard Error	Value	Standard Error	R-Square(COD)
Relative Humidity	ALL	34.31	6.23	-0.40	0.08	0.28
	ALL North of 65S	46.36	6.57	-0.56	0.08	0.49
	ALL South of 65S	8.35	12.49	-0.08	0.15	0.01
	SOE IX North of 65S	57.40	6.15	-0.64	0.08	0.77
	SOE X North of 65S	48.66	8.28	-0.64	0.11	0.61
	ALL SOE X	53.37	8.93	-0.71	0.12	0.51
	ALL SOE IX	42.72	6.54	-0.45	0.08	0.51
	Uemura All	54.12	4.27	-0.58	0.05	0.66
	Uemura North of 65S	55.71	5.82	-0.61	0.08	0.62
Sea Surface Temperature	ALL	-1.58	1.15	0.56	0.10	0.31
	ALL North of 65S	-4.83	1.46	0.74	0.11	0.52
	ALL South of 65S	0.59	2.06	1.50	1.81	0.03
	SOE IX North of 65S	-5.54	2.63	0.84	0.16	0.56
	SOE X North of 65S	-4.18	1.76	0.56	0.16	0.35
	ALL SOE X	-2.19	1.62	0.43	0.18	0.14
	ALL SOE IX	-0.36	1.60	0.58	0.12	0.42
	Uemura All	4.13	0.98	0.79	0.12	0.43
	Uemura North of 65S	3.43	1.35	0.85	0.13	0.53
Wind Speed	ALL	9.40	1.97	-0.47	0.12	0.18
	ALL North of 65S	11.68	2.54	-0.53	0.14	0.24
	ALL South of 65S	7.74	3.22	-0.55	0.25	0.19
	SOE IX North of 65S	15.16	3.35	-0.61	0.20	0.31
	SOE X North of 65S	5.93	3.67	-0.33	0.19	0.11
	ALL SOE X	6.08	2.96	-0.38	0.17	0.13
	ALL SOE IX	11.58	2.51	-0.47	0.17	0.20

Table 3. Slope, intercept and r^2 of the linear regression equations between observed and modelled $\delta^{18}O$ and d-excess for the best fit models for samples collected north of 65S

Observed vs Modelled		Intercept		Slope		Statistics	
		Value	Standard Error	Value	Standard Error	Adj. R-Square	Root-MSE (SD)
$\delta^{18}O$ All	UCG MJ 0.8	-8.88	0.57	0.18	0.03	0.28	1.15
	UCG CD 0.6	-9.06	0.59	0.17	0.04	0.26	1.20
	TCG MJ 0.6	-9.42	0.57	0.19	0.03	0.30	1.15
	TCG CD 0.7	-9.15	0.55	0.19	0.03	0.32	1.12
$\delta^{18}O$ North of 65S	UCG MJ 0.8	-6.45	0.89	0.34	0.06	0.38	0.84
	UCG CD 0.6	-6.50	0.91	0.34	0.06	0.38	0.86
	TCG MJ 0.6	-7.02	0.91	0.34	0.06	0.38	0.86
	TCG CD 0.7	-6.89	0.91	0.34	0.06	0.37	0.86
d-excess All	UCG MJ 0.8	-0.94	0.64	0.47	0.07	0.39	5.08
	UCG CD 0.6	-0.94	0.64	0.47	0.07	0.39	5.07
	TCG MJ 0.6	-6.46	0.75	0.58	0.08	0.41	6.00
	TCG CD 0.7	-7.39	0.71	0.55	0.08	0.41	5.66
d-excess North of 65S	UCG MJ 0.8	-0.35	0.63	0.60	0.07	0.63	4.07
	UCG CD 0.6	-0.36	0.63	0.60	0.07	0.63	4.06
	TCG MJ 0.6	-4.93	0.72	0.74	0.08	0.67	4.67
	TCG CD 0.7	-5.85	0.68	0.70	0.07	0.66	4.41

Supplementary document accompanying the manuscript 'Craig-Gordon model validation using stable isotope ratios in water vapor over the Southern Ocean'

Contents

1 Sample collection and isotopic analysis

Atmospheric moisture was sampled using cryogenic cold trap, which is custom-made using pyrex tubes where atmospheric vapor was condensed with the help of a freezing mixture of liquid Nitrogen and Ethanol; maintained the temperature at ≈ -80°C. First, the inlet was connected to the Poly vinyl chloride (PVC) tube which was set at the forecastle of the ship at two different heights as mentioned above. The outlet of the glass trap was connected to a vacuum pump which is maintained at a flow rate of ≈ 250 ml/min. The line was flushed using the pump for at least ≈ 15 Min's before starting the collection process to avoid any sort of residual ambient air inside the tubing and the trap. An Ultra Torr connector (Swagelok) was connected from PVC tubing to the glass flask and from glass trap to the vacuum pump. The sampling time required for generating appreciable amount (2-3ml) of condensed water for isotopic analysis was ≈ 3 to 6 hours depending on the sampling location with greater sampling time at higher latitudes. After the sampling is done both ends of the glass flask was sealed using Parafilm to avoid any air inclusion inside the flask. Atmospheric moisture, condensed inside the cold trap as ice, was allowed to melt at room temperature (≈ 15-20°C) and then transferred into 5 ml polyethylene storage vials. The samples were stored at 4°C. A similar setup for water vapor sampling was presented in the earlier studies Rahul et al. (2016, 2018).

Surface water samples were collected form Conductivity Temperature Depth (CTD) rosette when it was deployed and from a bucket thermometer used for measuring the sea surface temperature. Surface water samples were collected in 50ml High-Density Polyethylene air tight bottles.

All these samples were shipped to Bangalore for isotopic analysis and the measurements were carried out at the Centre for Earth Sciences, Indian Institute of Science, Bangalore. The protocol followed for the analysis of the gases after equilibration using a Finnigan Gas-bench II attached to a MAT 253 mass spectrometer is described in the (Rangarajan and Ghosh, 2011). For oxygen isotope analysis $200\mu L$ of water was transferred into an exetainer vial capped with butyl rubber septa and equilibrated with gas mixture 3% CO2+97% He for a period of 20 hours. For hydrogen isotopes, the water sample was equilibrated with gas mixture of 3% H2+97% He in presence of platinum catalyst (Hokko bead sticks) for a period of 80mins. The isotope ratios are expressed in ‰ using the standard δ notation relative to Vienna Standard Mean Ocean Water (VSMOW). Internal laboratory standards (OASIS-WWW, OASIS-LDK and OASIS-VOULEP) calibrated against the international water standards (VSMOW, Standard Light Antarctic Precipitation, and Greenland Ice Sheet Project) available from International Atomic Energy Agency in Vienna, were used to determine the accuracy and precision of the analysis. To account for intra batch calibration and drift correction, additional internal laboratory standards were measured in a batch. The overall analytical uncertainty on the measurements ($\pm 1\sigma$), as determined from replicate measurements of internal laboratory standards, were respectively $\pm 1.0‰$ and $\pm 0.1‰$ for δ^2H and $\delta^{18}O$. Isotopic values are reported here with one standard deviation.

2 Meteorological measurements

Atmosphere readings were taken via multiple instruments on-board the ocean research vessel SA Agulhas. Relative Humidity was calculated from the Psychrometric charts with the help of dry bulb and wet bulb temperature readings from sling Psychrometer with a range of -5°C to +50°C and a least count of 0.5°C . Air temperature, Atmospheric Pressure, Wind's magnitude and Direction, GPS were logged from AWS (Automatic Weather Station) installed on board the ship. Salinity was measured using an Auto Salino Meter (Tsurumi Seiki Co. Ltd, Japan. Salinity values are expressed in the 1978 Practical Salinity Scale (PSU) (PSS-78) with a precision of ±0.005 PSU. Sea Surface Temperature (SST) was measured using a bucket thermometer (Theodor Friedrichs and Co, Germany; accuracy ± 0.2°C).

3 Supplementary figures and tables

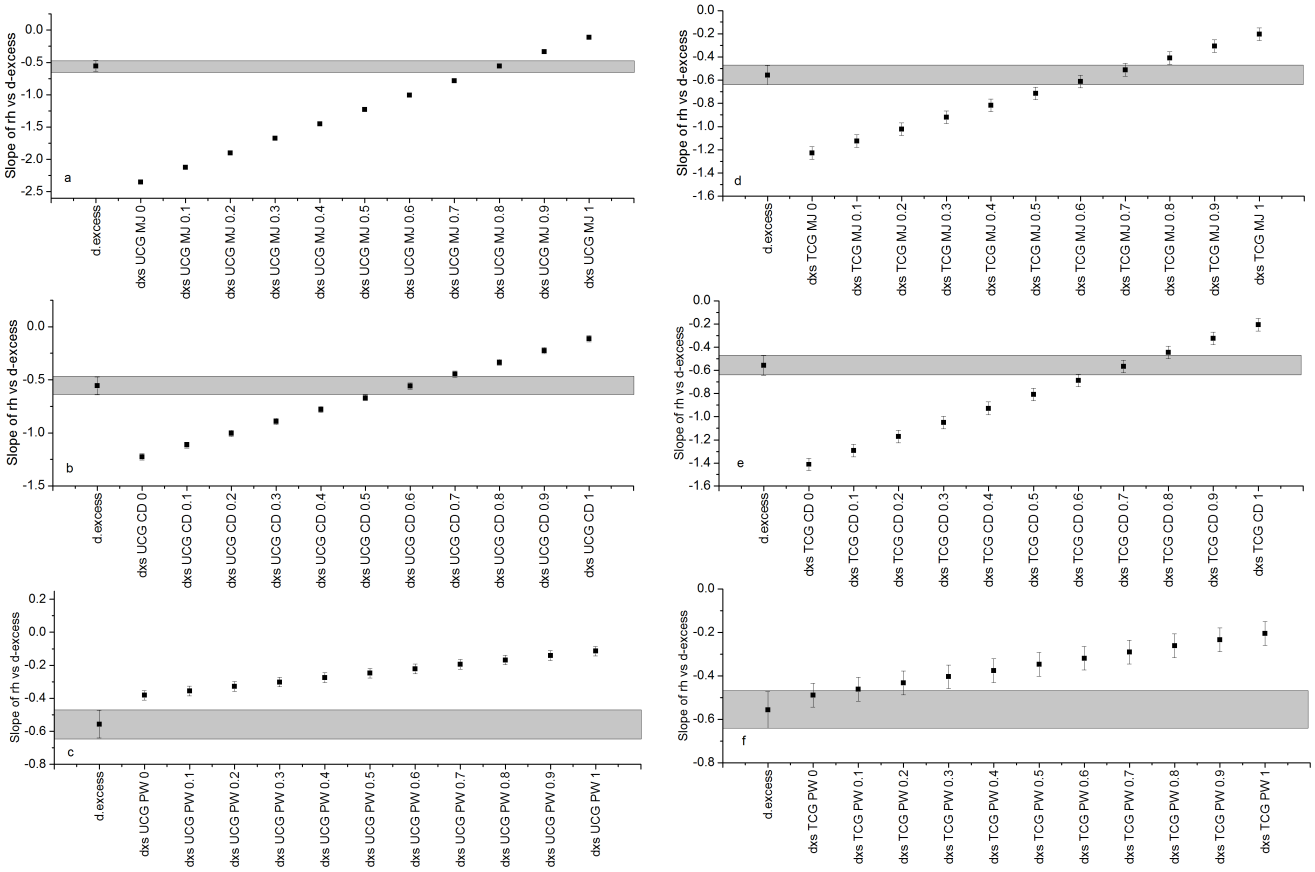

Figure 1. (S) Slope of the relative humidity vs d-excess for the UCG (a-c) and the TCG (d-f) model runs (filled black squares) and the observed value (grey band).

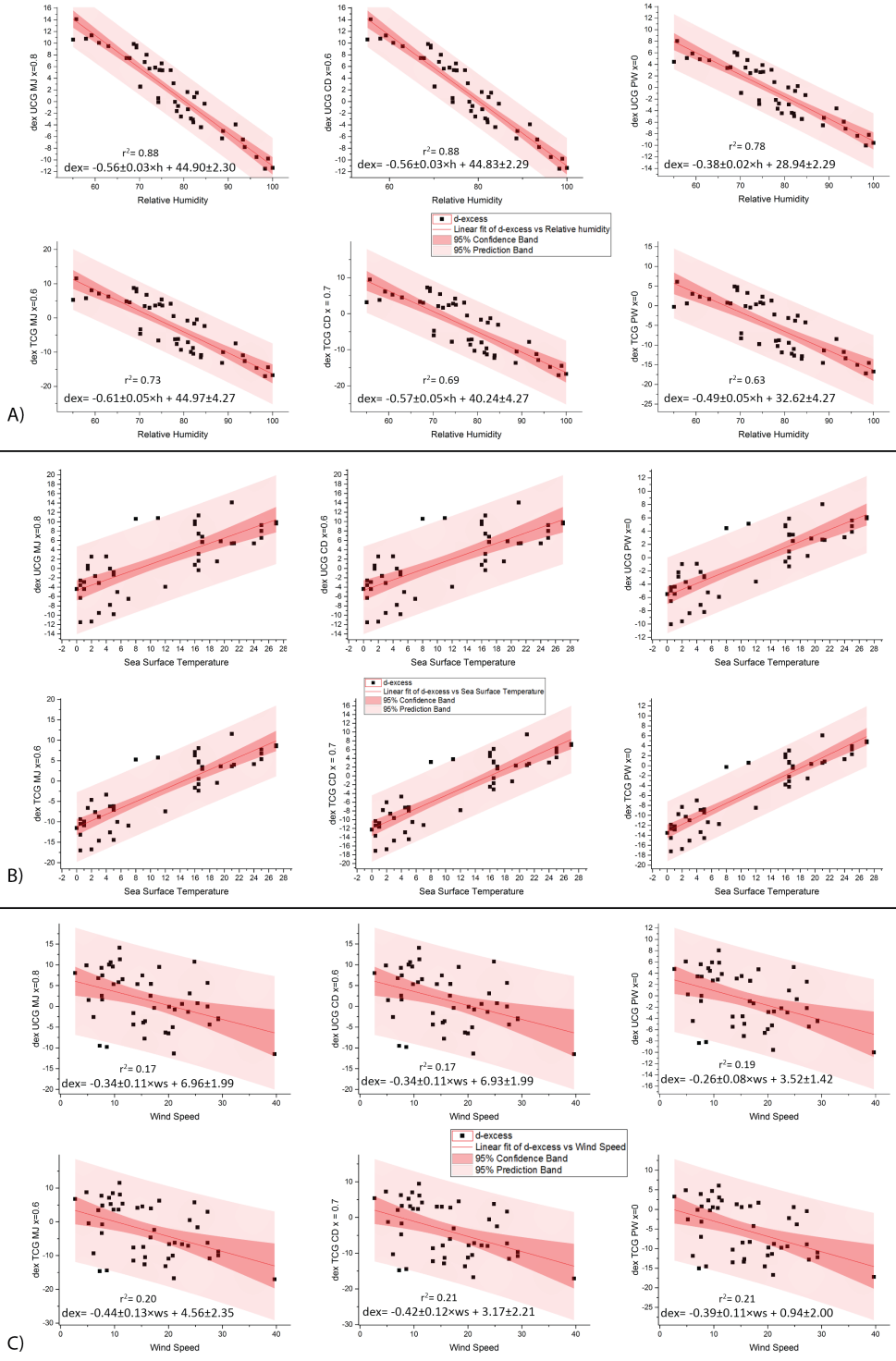

Figure 2. (S) Linear regression equations between relative humidity (A), sea surface temperature (B) and wind speed (C) and the d-excess of the best-fit model runs. The dark and light pink shaded regions depict the 95% confidence bands and 95% prediction bands respectively.

Table 1. (S) Slope, intercept and r^2 of the linear regression equations between meteorological parameters (relative humidity, sea surface temperature and winds speed) and $\delta^{18}O$ for different sample classifications. Also listed are the regression parameters for the data from Uemura et al. (2008)

Met. vs $\delta^{18}O$	Classification	Intercept		Slope		Statistics
		Value	Standard Error	Value	Standard Error	R-Square(COD)
Relative Humidity	ALL	-11.43	3.43	-0.06	0.04	0.03
	ALL North of 65S	-15.49	2.04	0.02	0.03	0.01
	ALL South of 65S	-11.05	5.11	-0.12	0.06	0.15
	SOE IX North of 65S	-12.37	2.59	-0.02	0.03	0.01
	SOE X North of 65S	-18.95	3.39	0.06	0.04	0.07
	Uemura All	-20.61	2.81	0.05	0.04	0.02
Sea Surface Temperature	ALL	-18.43	0.53	0.27	0.05	0.33
	ALL North of 65S	-15.47	0.40	0.12	0.03	0.27
	ALL South of 65S	-19.38	0.71	-2.37	0.62	0.41
	SOE IX North of 65S	-15.30	0.70	0.12	0.04	0.26
	SOE X North of 65S	-15.52	0.51	0.11	0.05	0.19
	ALL SOE X	-16.82	0.42	0.19	0.05	0.33
	ALL SOE IX	-21.07	0.96	0.41	0.07	0.51
	Uemura All	-17.40	0.46	0.19	0.05	0.16
Wind Speed	ALL	-17.85	1.01	0.10	0.06	0.04
	ALL North of 65S	-12.74	0.60	-0.09	0.03	0.13
	ALL South of 65S	-23.76	1.40	0.25	0.11	0.21
	SOE IX North of 65S	-12.62	0.77	-0.07	0.05	0.11
	SOE X North of 65S	-13.05	0.98	-0.09	0.05	0.12
	ALL SOE X	-16.66	0.93	0.06	0.05	0.03
	ALL SOE IX	-18.77	1.80	0.14	0.12	0.04

Table 2. (S) Slope, intercept and r^2 of the linear regression equations between meteorological parameters (relative humidity, sea surface temperature and winds speed) and $\delta^2 H$ for different sample classifications. Also listed are the regression parameters for the data from Uemura et al. (2008)

Met. vs $\delta^2 H$	Classification	Intercept		Slope		Statistics
		Value	Standard Error	Value	Standard Error	R-Square(COD)
Relative Humidity	ALL	-57.14	27.50	-0.90	0.35	0.09
	ALL North of 65S	-77.52	18.79	-0.42	0.24	0.06
	ALL South of 65S	-41.57	22.20	-0.77	0.27	0.27
	SOE IX North of 65S	-102.94	28.84	-0.18	0.38	0.01
	SOE X North of 65S	-133.31	30.61	0.10	0.41	0.00
	Uemura All	-110.71	22.14	-0.16	0.28	0.00
Sea Surface Temperature	ALL	-149.02	3.84	2.76	0.34	0.49
	ALL North of 65S	-128.58	2.78	1.68	0.20	0.61
	ALL South of 65S	-127.93	5.09	1.76	0.31	0.60
	SOE IX North of 65S	-128.31	3.31	1.41	0.30	0.50
	SOE X North of 65S	-136.73	2.72	1.95	0.30	0.55
	ALL SOE X	-168.91	7.05	3.88	0.53	0.63
	ALL SOE IX	-154.43	5.43	-17.47	4.77	0.39
	Uemura All	-135.09	2.99	2.28	0.36	0.41
Wind Speed	ALL	-133.39	8.50	0.36	0.51	0.01
	ALL North of 65S	-90.28	5.20	-1.24	0.29	0.29
	ALL South of 65S	-85.84	6.89	-1.19	0.41	0.29
	SOE IX North of 65S	-98.47	7.54	-1.04	0.40	0.23
	SOE X North of 65S	-127.16	7.58	0.07	0.43	0.00
	ALL SOE X	-138.60	15.43	0.63	1.01	0.01
	ALL SOE IX	-182.36	11.09	1.49	0.85	0.13

4 Data used in this study

Table 3. (S) SOE-IX meteorological data, water vapor and surface water isotopic composition

Date	**Lon**	**Lat**	**Tair** (^0C)	**Atm. Pres.** ($mbar$)	**Rel. Hum.** (%)	**Wind Speed** (m/s)	**SST** (^0C)	$\delta^{18}O$ (‰)	δ^2H (‰)	**d-excess** (‰)	**Sal.** (PSU)	$\delta^{18}O_{SW}$ (‰)
08/01/2017	57.50	-27.38	29.60	1015.80	69.31	9.68	27.0	-11.97	-83.04	12.71	35.59	
08/01/2018	57.52	-28.66	29.20	1014.80	68.69	4.80	27.0	-12.00	-80.79	15.17	35.50	
09/01/2017	57.49	-31.53	26.13	1016.50	69.31	7.58	25.0	-11.92	-82.11	13.22	35.54	0.31
09/01/2017	57.50	-32.26	24.13	1016.50	77.01	14.25	24.0	-12.16	-84.65	12.66	35.57	
09/01/2017	57.51	-33.44	19.83	1018.67	75.15	9.82	21.0	-12.22	-87.82	9.98	35.41	
10/01/2017	57.50	-35.38	21.50	1019.67	73.54	10.75	19.5	-12.29	-95.66	2.64	35.47	0.33
10/01/2017	57.51	-36.43	21.17	1017.67	82.94	5.20	19.0	-10.86	-82.74	4.16	35.46	
11/01/2017	57.87	-39.11	13.88	1018.25	72.25	27.25	17.0	-14.62	-104.60	12.36	35.58	
12/01/2017	58.41	-40.07	13.67	1027.83	60.86	9.00	16.0	-15.57	-107.66	16.89	35.41	
12/01/2017	57.94	-40.08	12.38	1028.00	67.06	7.75	16.5	-15.91	-109.99	17.33	35.51	
14/01/2017	58.52	-40.09	17.40	1017.80	82.36	25.40	16.0	-11.96	-91.18	4.52	35.36	0.38
13/01/2017	57.99	-40.21	13.00	1025.00	59.18	11.00	16.5	-14.88	-100.35	18.65	35.37	
15/01/2017	59.46	-41.38	14.17	1022.00	67.80	15.17	16.5	-14.37	-96.94	18.03	35.47	0.35
16/01/2017	61.15	-43.67	16.53	1023.83	71.16	7.00	17.0	-14.78	-101.41	16.85	35.49	-0.26
16/01/2017	62.72	-45.46	11.67	1012.33	91.67	15.33	12.0	-12.37	-100.60	-1.60	35.52	
17/01/2017	64.00	-47.02	7.33	1003.33	93.33	20.00	7.0	-15.19	-129.06	-7.57	33.72	-0.12
18/01/2017	64.10	-49.02	5.60	1008.60	88.86	20.80	5.5	-13.97	-118.99	-7.20	33.52	-0.12
19/01/2017	64.17	-51.05	5.45	1011.67	78.70	21.17	5.0	-14.40	-117.37	-2.18	33.80	-0.07
19/01/2017	67.00	-51.73	4.79	1009.29	98.97	8.57	5.0	-12.97	-106.26	-2.52	33.69	
20/01/2017	68.49	-54.01	4.54	1006.57	93.73	15.57	4.5	-12.68	-101.07	0.37	33.87	0.05
21/01/2017	69.29	-57.40	4.00	996.25	96.39	7.25	3.0	-13.39	-101.24	5.90	33.89	0.03
22/01/2017	70.08	-61.95	0.98	970.20	100.00	21.00	2.0	-19.46	-162.93	-7.26	33.61	-0.07
23/01/2017	68.34	-64.00	0.14	976.17	98.31	39.67	0.5	-14.82	-126.91	-8.37	33.83	0.18
24/01/2017	74.01	-65.99	0.09	983.00	95.57	14.86	0.5	-20.35	-160.07	2.72	33.86	
25/01/2017	72.54	-67.96	-0.51	992.14	96.45	20.57	1.5	-22.62	-182.23	-1.28	33.79	-0.61
26/01/2017	74.01	-67.99	1.00	991.33	72.19	7.67	1.5	-22.79	-177.95	4.41	33.43	
26/01/2017	74.00	-68.00	-0.33	992.00	83.67	12.00	1.5	-19.94	-154.85	4.66	33.21	
31/01/2017	76.00	-68.00	-1.75	978.00	94.23	5.83	1.5	-24.86	-193.54	5.31	32.73	
27/01/2017	74.05	-68.02	1.08	990.00	65.92	5.67	1.5	-23.33	-182.05	4.56	33.38	
30/01/2017	76.12	-68.04	-0.50	988.50	84.14	14.25	1.0	-22.17	-174.22	3.11	32.77	
27/01/2017	73.93	-68.21	0.12	988.40	80.13	8.20	2.0	-27.06	-221.38	-4.87	32.42	
28/01/2017	74.01	-68.60	-2.10	987.00	90.36	5.40	2.0	-27.47	-216.45	3.28		
31/01/2017	75.90	-69.19	-0.92	983.67	100.00	12.67	2.5	-24.25	-184.09	9.94	33.74	
01/02/2017	76.05	-69.34	0.33	991.33	97.92	7.33	0.0	-27.14	-211.65	5.46	32.07	
01/09/2018	74.73	-66.78	0.12	978.42	78.87	25.04	0.0	-17.54	-131.63	8.72	32.73	-0.57
01/02/2018	73.31	-66.80	0.74	989.95	76.64	8.75	0.0	-18.48	-142.40	5.41	33.37	-0.69

Table 4. (S) SOE-X meteorological data, water vapor and surface water isotopic composition

Date	**Lon**	**Lat**	**Tair** (^0C)	**Atm. Pres.** ($mbar$)	**Rel. Hum.** (%)	**Wind Speed** (m/s)	**SST** (^0C)	$\delta^{18}O$ (‰)	δ^2H (‰)	**d-excess** (‰)	**Sal.** (PSU)	$\delta^{18}O_{SW}$ (‰)
12/10/2017	57.56	-21.98	26.13	1015.50	75.00	11.50		-12.34	-94.50	4.20		
12/11/2017	57.79	-26.80	28.55	1012.70	71.60	2.70	25.0	-11.46	-88.03	3.61	35.41	0.53
12/12/2017	58.00	-31.05	21.53	1016.00	74.53	16.76	21.5	-12.87	-101.43	1.52	35.42	0.77
13/12/17	58.20	-35.24	19.00	1015.00	55.75	10.93	21.0	-15.58	-110.07	14.54	35.56	0.36
14/12/17	58.49	-39.84	18.00	1007.13	80.82	7.72	16.5	-12.21	-98.43	-0.77	35.51	0.36
15/12/17	57.49	-39.99	14.46	995.03	84.68	17.36	16.5	-13.54	-100.92	7.39	33.84	0.61
16/12/17	58.80	-40.18	14.05	1015.04	63.00	18.29	16.0	-15.56	-110.40	14.11	35.47	0.28
17/12/17	58.38	-40.19	16.93	1016.80	77.68	23.94	16.5	-12.11	-97.43	-0.54	35.46	
18/12/17	60.50	-42.89	9.33	1011.52	57.95	24.82	11.0	-15.52	-115.67	8.51	33.95	
19/12/17	62.63	-45.69	8.07	1015.17	55.04	9.29	8.0	-16.56	-118.22	14.29	34.38	0.08
20/12/17	64.35	-48.07	6.94	991.67	80.92	23.65	5.0	-13.62	-112.24	-3.28	33.90	-0.41
21/12/17	63.85	-50.78	4.52	972.07	78.00	27.25	4.5	-14.31	-120.64	-6.12	33.81	-0.55
22/12/17	65.58	-53.07	4.79	970.60	70.21	7.64	4.0	-14.58	-121.16	-4.54		-0.02
23/12/17	68.23	-54.02	2.26	981.60	82.06	29.24	3.0	-15.81	-132.28	-5.76	33.90	0.02
24/12/17	69.03	-56.43	2.80	993.74	78.40	13.49	2.5	-14.05	-118.57	-6.19	33.95	-0.01
25/12/17	70.14	-58.03	3.18	1002.36	70.17	16.68	2.0	-14.44	-111.16	4.33	33.92	-0.57
25-26/12/17	70.12	-59.05	1.80	1002.17	82.14	15.67	0.5	-13.58	-108.05	0.60	33.08	-0.39
26/12/17	71.59	-59.99	1.21	993.15	83.82	13.50	0.0	-13.35	-112.80	-5.97	33.61	-0.48
26/12/17	71.14	-61.06	0.14	984.87	88.64	19.45	0.5	-13.93	-120.74	-9.32	33.68	-0.51
27/12/17	70.90	-61.66	1.19	985.72	79.35	6.12	0.5	-15.74	-129.25	-3.30	33.71	-0.20
17-18/1/18	57.49	-61.99	2.80	986.17	74.25	20.14	1.5	-15.39	-130.38	-7.28	33.70	
28/12/17	69.99	-63.01	-1.02	990.34	74.22	22.52	1.5	-21.18	-163.28	6.18	33.63	-0.59
17/01/18	57.52	-63.05	1.16	974.27	81.60	29.23	1.0	-16.63	-141.06	-8.01	33.49	
16-17/1/18	57.42	-64.01	1.90	969.20	83.90	27.63	1.0	-15.02	-130.43	-10.24	33.20	-0.22
14/01/18	66.99	-65.49	-0.70	971.30	79.66	17.03	0.0	-15.40	-121.20	2.00		-0.35
16/01/18	57.85	-65.51	1.34	967.24	84.00	27.02	1.0	-15.70	-141.37	-15.73	33.57	-1.05
30/12/17	74.91	-65.51	-0.36	978.48	76.16	6.21	0.0	-18.88	-148.91	2.15	33.39	-0.62
01/10/2018	68.81	-65.51	0.31	980.96	61.30	4.00	-0.5	-20.40	-151.04	12.15	33.69	-3.45
31/12/17	73.84	-65.52	-0.40	984.47	74.00	14.10	0.0	-18.33	-152.82	-6.18	33.51	-1.16
31/12/17-1/1/18	72.67	-65.54	-0.25	988.00	81.50	16.40	-1.0	-16.77	-157.86	-23.71	33.61	-0.80
15/01/18	57.26	-65.58	-0.33	973.95	72.66	11.08	0.5	-19.64	-155.75	1.40	33.48	
29-30/12/17	74.79	-66.35	-1.35	982.00	62.50	7.00	-0.5	-21.11	-161.02	7.88	32.99	-0.64
01/07/2018	74.98	-66.43	1.86	981.77	63.53	4.88	0.0	-18.17	-137.79	7.59	32.73	
01/01/2018	73.00	-66.45	0.90	987.10	77.67	5.60	-0.5	-17.65	-144.89	-3.72	32.73	-0.33
01/09/2018	74.73	-66.78	0.12	978.42	78.87	25.04	0.0	-17.54	-131.63	8.72	32.73	-0.57
01/02/2018	73.31	-66.80	0.74	989.95	76.64	8.75	0.0	-18.48	-142.40	5.41	33.37	-0.69

References

Rahul, P., Ghosh, P., Bhattacharya, S., and Yoshimura, K.: Controlling factors of rainwater and water vapor isotopes at Bangalore, India: Constraints from observations in 2013 Indian monsoon, Journal of Geophysical Research: Atmospheres, 121, 2016.

Rahul, P., Prasanna, K., Ghosh, P., Anilkumar, N., and Yoshimura, K.: Stable isotopes in water vapor and rainwater over Indian sector of Southern Ocean and estimation of fraction of recycled moisture, Scientific reports, 8, 2018.

Rangarajan, R. and Ghosh, P.: Role of water contamination within the GC column of a GasBench II peripheral on the reproducibility of 18O/16O ratios in water samples, Isotopes in environmental and health studies, 47, 498–511, 2011.

Uemura, R., Matsui, Y., Yoshimura, K., Motoyama, H., and Yoshida, N.: Evidence of deuterium excess in water vapor as an indicator of ocean surface conditions, Journal of Geophysical Research: Atmospheres, 113, 2008.